



NEAR EAST UNIVERSITY

INSTITUTE OF GRADUATE STUDIES

DEPARTMENT OF BIOMEDICAL ENGINEERING

GELLAN GUM-BASED HYDROGELS FOR CELL CULTURING

PhD THESIS

MTHABISI TALENT GEORGE MOYO

NICOSIA

2025

**MTHABISI TALENT
GEORGE MOYO**

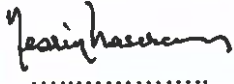
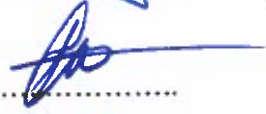
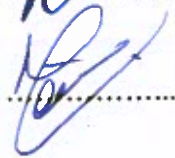
**GELLAN GUM-BASED HYDROGELS FOR
CELL CULTURING**

PhD THESIS

**NEU
2025**

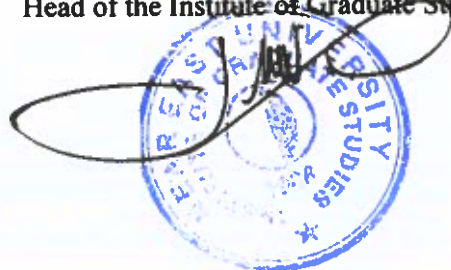
Approval

We certify that we have read the thesis submitted by Mthabisi Talent George Moyo titled "Gellan gum-based hydrogels for stem cell culturing" and that in our combined opinion it is fully adequate, in scope and quality, as a thesis for the degree of Doctor of Philosophy in Biomedical Engineering.

Examining Committee	Name-Surname	Signature
Head of the Committee:	Prof. Dr. Elvan Yilmaz	
Committee Member*:	Prof. Dr. Nesrin Hasirci	
Committee Member*:	Assoc. Prof. Dr. Sileyman Arir	
Committee Member*:	Prof. Dr. H. Seda Vatansuer	
Supervisor:	Prof. Dr. Arac Tulcu	
Co-supervisor:	Prof. Dr. Terin Adali	
Approved by the Head of the Department		 11.106.2025 Assoc. Prof. Dr. Sileyman Arir Title, Name-Surname Head of the Department

Approved by the Institute of Graduate Studies

11.106.2025
Prof. Dr. Kemal Hüsnü Can Başer
Head of the Institute of Graduate Studies



Declaration of ethical principles

I hereby declare that all information, documents, analysis and results in this thesis have been collected and presented according to the academic rules and ethical guidelines of the Institute of Graduate Studies, Near East University. I also declare that as required by these rules and conduct, I have fully cited and referenced information and data that are not original to this study.

Mthabisi Talent George Moyo
Name and Surname of the Student

.11./06./2025

Day/Month/Year

Acknowledgements

I would like to express my deepest gratitude to those who have supported and guided me throughout the process of writing this thesis.

First and foremost, I am profoundly grateful to my co-supervisor, Prof. Dr Terin Adali, whose expertise, patience, and unwavering support have been invaluable. Your insightful feedback and encouragement were crucial in shaping this work and pushing me to achieve my best.

I also wish to thank the committee members for their constructive critiques and thoughtful suggestions. Your input greatly enhanced the quality of this research, and I deeply appreciate your time and effort.

A special thank you goes to my colleagues and friends, for their camaraderie, discussions, and moral support. Your encouragement kept me motivated and helped me navigate the challenges of this journey.

To my family, your constant love, patience, and understanding provided the foundation I needed to complete this thesis. Your belief in me has been a source of strength throughout this process.

Thank you all for your significant contributions to this work. It would not have been possible without your support.

Sincerely,

Mthabisi Talent George Moyo

Abstract

Gellan Gum-Based Hydrogels for Cell Culturing

Mthabisi Talent George Moyo

PhD, Department of Biomedical Engineering

February 2025, 84 Pages

The present study deals with the possible role of gellan gum-based hydrogels with sodium alginate and silk fibroin in supporting mouse embryonic stem cells (mESCs) and interacting with blood. Hydrogels were prepared with Gellan gum concentrations of 0.3%, 0.5%, 0.75%, and 1% and characterized for mechanical properties, swelling capacity, cytocompatibility using LDH and MTT assays, and blood compatibility according to ISO 10993 standards. Swelling kinetics were tested in phosphate (PBS) and acetic (ABS) buffer solutions. Gellan gum–sodium alginate hydrogels showed approximately 10% higher swelling in PBS and reduced swelling in ABS. The 0.5% and 0.75% formulations exhibited optimal cytocompatibility for mESC and fibroblast (STO) cultures. Test for hemocompatibility revealed that the formulation with a gellan gum concentration of 0.3, 0.5, and 0.75% resulted in a normal response. Meanwhile, the hemolysis and thrombogenic effects significantly increased when the concentration was 1%. DSC analysis showed that silk fibroin improved the flexibility of the scaffold by reducing the peak temperature, while sodium alginate enhanced the thermal stability of the scaffold. Incorporating sodium alginate led to smoother surfaces according to the SEM analysis, while silk fibroin contributed to increased roughness, and this was much more pronounced at higher gellan gum concentrations in the blends. These findings demonstrate the excellent biocompatibility and hemocompatibility of gellan gum with sodium alginate and gellan gum with silk fibroin hydrogels with potential use in tissue engineering and blood-contact applications.

Keywords: *Gellan Gum; Silk fibroin; Sodium alginate; Hydrogels; Mouse embryonic stem cells*

Özet

Hücre Kültürü için Gellan Zamkı Bazlı Hidrojeller

Mthabisi Talent George Moyo

Doktora, Biyomedikal Mühendisliği Bölümü

Şubat 2025, 84 Sayfa

Mevcut çalışma, sodyum aljinat ve ipek fibroin içeren gellan zamkı bazlı hidrojellerin fare embriyonik kök hücrelerini (mESC) destekleme ve kanla etkileşime girmedeki olası rolüyle ilgilenmektedir. Hidrojeller, %0,3, %0,5, %0,75 ve %1'lik Gellan zamkı konsantrasyonlarıyla hazırlanmış ve mekanik özellikler, şişme kapasitesi, LDH ve MTT analizleri kullanılarak sito-uyumluluk ve ISO 10993 standartlarına göre kan uyumluluğu açısından karakterize edilmiştir. Şişme kinetiği fosfat (PBS) ve asetik (ABS) tampon çözeltilerinde test edilmiştir. Gellan zamkı-sodyum aljinat hidrojelleri, PBS'de yaklaşık %10 daha fazla şişme ve ABS'de daha az şişme göstermiştir. %0,5 ve %0,75 formülasyonları, mESC ve fibroblast (STO) kültürleri için optimum sito-uyumluluk göstermiştir. Hemokompatibilite testi, %0,3, %0,5 ve %0,75'lik bir gellan gum konsantrasyonuna sahip formülasyonun normal bir yanıtla sonuçlandığını ortaya koydu. Bu arada, konsantrasyon %1 olduğunda hemoliz ve trombojenik etkiler önemli ölçüde arttı. DSC analizi, ipek fibroinin tepe sıcaklığını azaltarak iskelenin esnekliğini iyileştirdiğini, sodyum aljinatın ise iskelenin termal kararlılığını artırdığını gösterdi. SEM analizine göre, sodyum aljinatın dahil edilmesi daha pürüzsüz yüzeylere yol açarken, ipek fibroini pürüzlülüğün artmasına katkıda bulundu ve bu, karışımlardaki daha yüksek gellan gum konsantrasyonlarında çok daha belirgindi. Bu bulgular, sodyum aljinatlı gellan gum ve ipek fibroinli gellan gum hidrojellerinin mükemmel biyouyumluluğunu ve hemokompatibilitesini ve doku mühendisliği ve kan teması uygulamalarında potansiyel kullanımını göstermektedir.

Anahtar Kelimeler: *Gellan zamkı; İpek fibroin; Sodyum aljinat; Hidrojeller; Fare embriyonik kök hücreleri*

Table of contents

Approval	1
Declaration of ethical principles	2
Acknowledgements	3
Abstract	4
Table of contents	6
List of tables	8
List of figures	9
List of abbreviations	10

CHAPTER I

Introduction	11
1.1 Statement of problem	16
1.2 Purpose of the study	16
1.3 Research questions	16
1.4 Significance of the study	17
1.5 Limitations	17

CHAPTER II

Literature review	19
2.1 Regenerative medicine and tissue engineering	19
2.2 Biomaterials used in mESC culturing	19
2.3 Challenges the use of gellan gum	24
2.4 Hemocompatibility of biomaterials	25

CHAPTER III

3.1 Materials	27
3.2 Methods	27
3.2.1 Silk fibroin extraction and purification process	27
3.2.1.1 <i>Degumming process</i>	27
3.2.1.2 <i>Dissolution process</i>	28
3.2.1.3 <i>Dialysis</i>	28
3.2.2 Sodium alginate dissolution	29
3.2.3 Gellan gum dissolution	29
3.2.4 Hydrogel preparation	29
3.2.5 Swelling Kinetics	29
3.2.6 Lyophilization	30
3.2.7 Cell culture	31
3.2.8 Cell viability assay	32
3.2.9 Differential scanning calorimetry (DSC)	32
3.2.10 Scanning electron microscopy (SEM)	33
3.2.11 Blood biocompatibility	33

CHAPTER IV

Findings and discussion	37
4.1 Formulations of hydrogels	37
4.2 Swelling kinetics.	38
4.3 Cell culture.	39
4.4 MTT results	45
4.6 Differential scanning calorimetry(DSC)	48
4.7 Scanning electron microscopy (SEM).....	49
4.5 Hemocompatibility studies.....	51
4.5.1 Complete blood count assessment.....	51
4.5.2 Coagulation analysis.....	56
4.5.3 Quantitative hemolysis index analysis	57
4.5.4 Erythrocyte structural analysis and platelet adhesion assessment.....	58

CHAPTER V

Discussion.....	60
Conclusion and recommendations	68
REFERENCES.....	70
Similarity report	74
Hemocompatibility ethical approval.....	82
Figure 1 publishing license	83
Figure 2 publishing license	84

List of tables

Table 1 Biomaterials used In mESC culturing.....	22
Table 2 Formulated hydrogels and their compositions	37
Table 3 Complete blood count (CBC) analysis.....	53
Table 4 Coagulation analysis of test samples against controls	56
Table 5 Quantitative hemolysis index analysis.....	57

List of figures

Figure 1 Overview of standards and testing procedures for biomaterials.....	15
Figure 2 ISO 10993-4 hemocompatibility assay steps.....	34
Figure 3 Swelling ratio of gellan gum hydrogels in PBS (A, B) and ABS (C, D)....	38
Figure 4 Morphological changes in STO cells during culture.	39
Figure 5 Images of STO + mESC co-culture over time.....	40
Figure 6 Morphology of mESCs with hydrogels on day 1	42
Figure 7 Morphology of mESCs with hydrogels on day 4.	43
Figure 8 Morphology of mESCs with hydrogels on day 7.....	44
Figure 9 MTT Results for day 1, 4 and 7 of mESC ,CM and hydrogels.	46
Figure 10 LDH results for day 1, 4 and 7 of mESC ,CM and hydrogels.....	47
Figure 11 DSC thermograms	49
Figure 12 SEM images.....	50
Figure 13 Peripheral blood smears.....	59

List of abbreviations

ABS: Acid phosphate buffer solution

aPTT: Activated partial thromboplastin time

CBC: Complete blood count

ECM: Extracellular matrix

ESC: Embryonic stem cells

hESC: human Embryonic Stem Cells

LDH: Lactate Dehydrogenase

mESC: mouse Embryonic Stem Cells

MTT Assay: Methylthiazolyl Diphenyl Tetrazolium Bromide Assay

PBS: Phosphate buffer solution

PT: Prothrombin time

1. CHAPTER I

Introduction

A key element of the evolution of regenerative medicine and biomedical devices is biomaterials (Festas et al., 2020). Basic solutions to tissue engineering, drug delivery, and medical device development (Festas et al., 2020; Nii & Katayama, 2021). Biomaterials for such applications should demonstrate excellent biocompatibility—both cytocompatibility for regenerative medicine and hemocompatibility for blood-contacting devices (Bernard et al., 2018; Nalezinková, 2020). Hydrogels have emerged as promising candidates owing to their high water content biocompatibility, and ability to replicate the microenvironment of native tissue (Ho et al., 2022). However, their translation to the clinic is consistently hindered by a lack of understanding of their interactions with cells and blood components, particularly with compliance to strict ISO standards such as ISO 10993-4 and ISO 10993-5 (Sethi et al., 2024; Xu et al., 2022).

The practice of regenerative medicine aims to restore or regenerate injured tissue using biomaterials that interact with cells to facilitate tissue regeneration (Ntege et al., 2020). Biomaterials are also used by biomedical devices to provide structural support for applications like implants, stents, and wound dressings (Festas et al., 2020; (Moyo et al., 2024; Moyo & Adali, 2024)). Natural biomaterials like collagen, silk fibroin, and gellan gum have higher biocompatibility and bioactivity than synthetic biomaterials like poly(lactic-co-glycolic acid) and polyethylene glycol (Bhatia & Bhatia, 2016). Although biomaterials have benefits, the majority of them fail to meet rigorous cytocompatibility and hemocompatibility standards, and thus their clinical uses are restricted (Beilharz et al., 2024; Spataru et al., 2024).

Hydrogels are of special interest in tissue engineering and medical devices due to their ability to replicate native tissue water content (Akulo et al., 2022; Radulescu et al., 2022; Sanjanwala et al., 2024). Hydrogels as 3D scaffolds facilitate cell adhesion, proliferation, and differentiation with mechanical properties that can be tuned to regulate destined cell fates (Naahidi et al., 2017). Hydrogels may also be loaded with bioactive molecules, i.e., growth factors, for tissue regeneration. Hydrogels find application in contact lenses, wound dressings, drug patches, and bioengineered skin substitutes, among other medical device applications (Tsou et al., 2016). Hydrogels

find a basic application in regenerative medicine and medical technologies because of their versatility and biocompatibility (Naahidi et al., 2017).

Polysaccharide Gellan gum has attracted more interest in biomedical and regenerative medicine applications following the unexpected surge of its biocompatibility and gelation at low concentration levels (Morris et al., 2012; Moyo, Adali, & Tulay, 2024; Moyo & Adali, 2024.). There is no study on gellan gum hydrogels, specifically its hemocompatibility utilizing ISO 10993-4 standards (Moyo, Adali, & Edebal, 2024). Although research has been carried out on the gelation behavior and mechanical strength of the gels, some of the most important parameters such as coagulation, thrombosis, platelet activation, and immune response have been less studied (D. A. De Silva et al., 2013; Meng et al., 2013; Moyo, Adali, & Edebal, 2024).

For better hemocompatibility, hybrid hydrogels of gellan gum mixed with other biopolymers such as silk fibroin and sodium alginate have shown promising results (Moyo, Adali, & Edebal, 2024). Silk fibroin prevents fibrin deposition, while sodium alginate prevents platelet aggregation and clotting (Adalı & Uncu, 2016; Wang et al., 2023). Such synergy creates a hydrogel matrix that is more blood compatible, reducing the risk of immune activation. Additionally, the combination of gellan gum with silk fibroin and sodium alginate provides increased mechanical stability and simulates the biochemical nature of the ECM to provide an ideal environment for the culture of stem cells (Moyo, Adali, & Edebal, 2024).

ESCs are greatly valuable in research to study stem cell biology and biomaterial development due to their unique capacity for self-renewal and pluripotency (Rippon & Bishop, 2004). The ethical implications of using hESCs limit their use and prefer the use of mESCs as an alternative (Park et al., 2024; Roche & Grodin, 2000). mESCs share many biological features with hESCs and are now significant in developmental biology, disease modeling, and tissue engineering, particularly in assessing hydrogel biocompatibility (Koestenbauer et al., 2006).

The broader utility of these cells beyond that, mESCs are a significant benefit to scientists due to the fact that they have a high rate of proliferation. Their doubling time, after all, is only 12-15 hours, whereas it's 18-36 hours in the case of induced pluripotent

stem cells (iPSCs) (Guenther et al., 2010; Yabe et al., 2019). Although mESCs remain an invaluable resource for stem cell science, iPSCs are being increasingly considered an ethical alternative with viability (Kingham & Oreffo, 2013; Thanaskody et al., 2022). iPSCs offer comparable differentiation ability without circumventing ethical concerns when using embryonic cells (Thanaskody et al., 2022). The application of iPSCs will be likely to advance scientific research and public acceptance of stem cell research, as developments in regenerative medicine continue (Kingham & Oreffo, 2013).

One of the greatest challenges for stem cell research is to replicate the complex ECM environment that governs cell behavior (Gattazzo et al., 2014). Traditional 2D culture models fail to simulate the appropriate biochemical and mechanical stimulation for stem cell control (Jensen & Teng, 2020). Development of the 3D culture models has supplemented this chapter quite far by developing more naturalistic conditions such as the ECM, with substantial cell interaction support for regenerating tissues (Li & Kilian, 2015). The rising role of hydrogel-based biomaterials in regenerative medicine is seen in such developments that are at the forefront of tissue engineering. International Organization for Standardization (ISO) provides an acceptable protocol to determine the performance and safety of the biomaterials (Thangaraju & Varthya, 2022).

ISO 10993-5 specifies *in vitro* cytotoxicity tests in a standard manner to ensure that biomaterials do not induce toxic cell responses. In regenerative medicine and stem cell culture, its compliance should be in a rigorous manner to facilitate optimum microenvironment supply for proliferation and differentiation of cells (De Jong et al., 2020).

Of equal importance is hemocompatibility, or the capability of a material to come in contact with blood components in such a way that it does not result in an adverse reaction and hence be acceptable for use in contact with blood (Seyfert et al., 2002). Hemocompatibility is specifically dealt with under ISO 10993-4, wherein measurement of important parameters is the focus. Compliance with this standard is an important parameter in the development of biomaterials for blood-contacting applications as it eliminates the possibility of adverse hematological reactions (Standard, 2017).

By tackling cytocompatibility and hemocompatibility with methodical strategies, researchers can create biomaterials that achieve strict biomedical safety requirements while also promoting tissue formation, regenerative therapy, and medical device development. Harmonization of these standards with biomaterials research maximizes translation to the clinic, and the overall outcome is safer, more effective medical therapy (Murphy et al., 2020).

Apart from biocompatibility, there are other ISO standards that play significant parts in assessing biomaterials (International Organization for Standardization (ISO), 2018). They include sterilization standards for the removal of microorganisms from the materials, toxicology testing for assessing harmful impacts, and establishing physical and chemical properties to provide material integrity. Figure 1 presents these significant standards and test procedures, demonstrating how extensive testing forms the foundation of delivering biomaterials in line with regulatory requirements. Tests are required to ensure biomaterials are reproducible in performance in clinical practice, improve patient outcomes, and improve medical technology (International Organization for Standardization (ISO), 2018).

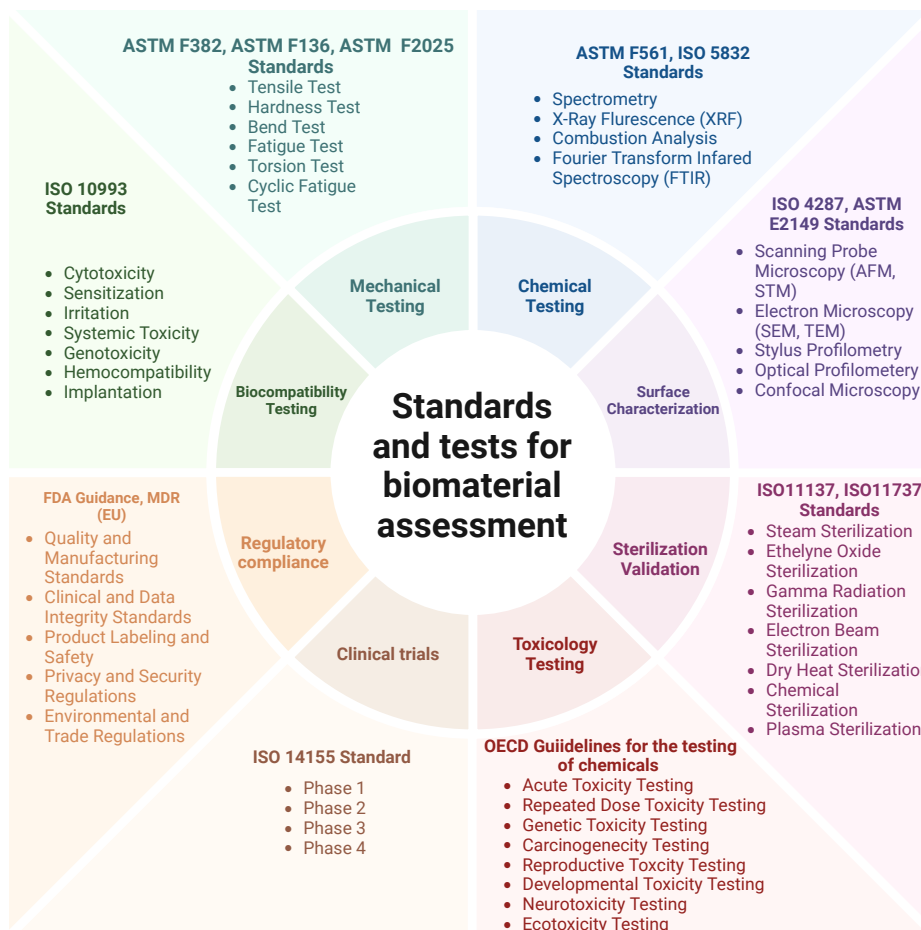


Figure 1
Summary of standards and testing protocols for biomaterials.

Hypotheses are formed that the synergistic combination of gellan gum with sodium alginate and separately with silk fibroin should promote the intercellular interaction as well as blood interaction, making it a suitable vehicle for mouse embryonic stem cell (mESC) culture as well as to ISO 10993-4 hemocompatibility standards. Hybrid hydrogels will mimic the ECM more effectively and promote the adhesion, growth, as well as differentiation of mESCs, while deleterious interactions with the constituents of blood will be minimized to the minimum.

Although gellan gum is promising, it has been studied sparingly for cytocompatibility with mESCs and hemocompatibility according to ISO 10993-4 standards. Moreover, the synergistic effects of using gellan gum combined with biomaterials such as sodium alginate as well as silk fibroin are yet to be extensively studied. Silk fibroin provides mechanical strength and provides bioactive signals, while sodium alginate has tunable stiffness through ionic crosslinking. Investigation

of these combinations is expected to provide insights into the way hybrid hydrogels should be optimized for hemocompatibility and stem cell culture.

1.1 Statement of problem

While there have been successful experiments conducted on gellan gum hydrogels, these still do not meet the entire criteria for both cytocompatibility and hemocompatibility, which limits their full application in regenerative medicine and in biomedical devices. Further, despite such promising results, there is very little work being carried out on how the gellan gum-derived hydrogels work in ESC and whether they meet. ISO 10993-4 standards, thus creating a gap which hinders their universal clinical application.

1.2 Purpose of the study

This study will evaluate the extent to which gellan gum hydrogels promote mESC growth and blood compatibility. The study will specifically examine the synergy of co-blending gellan gum with silk fibroin and with sodium alginate alone for improving biomimicry of the ECM, stem cell differentiation, and compatibility with the specifications of ISO 10993-4 hemocompatibility standards. This research is aimed at enhancing hydrogel development for application in both regenerative medicine and blood-contacting biomedical devices.

1.3 Research questions

- How does the inclusion of silk fibroin or sodium alginate into gellan gum hydrogels affect their cytocompatibility, hemocompatibility, and swelling response upon exposure to physiological conditions for culturing mESC?
- To what extent do gellan gum hydrogels with silk fibroin and sodium alginate satisfy ISO 10993-4 hemocompatibility standards and swell as predicted under physiological conditions?
- How are proliferation, differentiation of mESC, hemocompatibility, and swelling behavior under physiological conditions influenced by the changes in gellan gum concentration and incorporation of silk fibroin or sodium alginate?

- How do the morphology, thermal stability, and swelling properties of gellan gum hydrogels in physiological conditions influence their suitability for mESC culture and blood-contact biomedical devices??

1.4 Significance of the study

This research is directed towards filling the main knowledge gaps on the cytocompatibility of gellan gum with mESCs and hemocompatibility based on ISO 10993-4 guidelines. By exploring the synergistic impacts of gellan gum with silk fibroin, and separately blended with sodium alginate, this research supports the development of biomaterials in regenerative medicine and biomedical devices. The findings can be utilized to enhance the clinical applicability of these kinds of hydrogels and provide valuable insights into the future optimization and standardization of biomaterials.

1.5 Limitations

This study has several limitations that should be kept in mind while drawing conclusions about the data. For example, the research was conducted on particular gellan gum-based hydrogels. concentrations (0.3%, 0.5%, 0.75%, and 1%), which may not be able to cover the whole range of potential effective concentrations. The research was conducted using only mESC and mouse fibroblasts (STO), so there is limited scope for the data to be extrapolated to other cell types or human cells. Performed in controlled *in vitro* conditions, the study findings might not fully mimic the complexities of the *in vivo* environments, and thus doubts could be raised about the performance of the hydrogels in actual biological systems. The swelling kinetics were further tested only in phosphate buffer solution (PBS) and acetic buffer solution (ABS), potentially overlooking other pertinent physiological fluids. The thermal analysis, by Differential Scanning Calorimetry (DSC), would have been complemented with other characterization techniques to provide a better understanding of thermal behavior. Surface characteristics were examined using scanning electron microscopy (SEM), but techniques like atomic force microscopy would have provided more accurate surface data. Short-term assessment of

biocompatibility and mechanical properties in the work lacks long-term assessment, which is necessary for tissue engineering use.

2. CHAPTER II

Literature review

2.1 Regenerative medicine and tissue engineering

Tissue engineering is an emerging technology that revolves around the repair of injured tissues by using biocompatible scaffolds that facilitate cell growth and functioning naturally (Raghavendra et al., 2015). Stem cells are at the center of this technology yet are limited by ethical issues and paucity (Jin et al., 2019; Tsaryk et al., 2017).

Scientists such as Raghavendra et al., (2015) have overcome the limitation of tissue regeneration through the utilization of natural hydrogels as scaffolds. Their work not only indicated improvement in cell differentiation and viability but also examined hemocompatibility of the scaffold, thus ensuring that they were suitable for application in biomedicine. The scaffold is designed to promote maximum cell recruitment to the target tissue regeneration area. There, the cells are designed to grow, mature, and become tissue within the scaffold. Over time, the scaffold eventually dissolves away, and instead, new tissue forms to fill in its place.

Researchers Aamodt & Grainger, (2016) have surpassed the issue of tissue regeneration through natural hydrogels as scaffolds. They based their research on improving cell viability and differentiation along with hemocompatibility of scaffolds and hence establishing their potential for biomedical uses. The motivation behind this concept is fueled by the assumption that biomaterials derived from natural tissues, or ECM biomaterials, will achieve greater integration with host tissues than fully synthetic biomaterials.

These studies collectively emphasize the collaborative efforts in tissue engineering towards effective utilization of stem cells and advanced biomaterials for effective tissue regeneration. They also acknowledge the difficulties that scientists still face as the field of tissue engineering keeps developing.

2.2 Biomaterials used in mESC culturing

Scientists have explored a wide range of natural and synthetic biomaterials to recreate the 3D structure of the ECM and influence stem cell behavior. Materials like collagen, gelatin, hyaluronic acid hydrogels, fibrin, glycosaminoglycans, alginate, Matrigel, silk, and hydroxyapatite have been widely used to promote stem cell growth and differentiation, as highlighted in Table 1. Silk fibroin, gellan gum, and sodium alginate stand out because their mechanical and adhesive properties are strikingly like those found in the natural extracellular matrix, making them particularly valuable for various applications (Bhatia & Bhatia, 2016).

Alginate, a naturally derived anionic polysaccharide from brown algae, is widely used in tissue engineering and cell encapsulation due to its versatile properties (Andersen et al., 2015). The potential of purified alginic acid membranes and hydrogels for supporting the growth of cells and preserving certain cellular activities has been excellently established (Rastogi & Kandasubramanian, 2019; Wong et al., 2019). Naturally occurring sodium alginate is appreciated for its excellent biocompatibility, gelation capacity, nontoxicity, biodegradability, and simplicity to modify. Because of these favorable traits, alginate is extremely well-suited for a variety of applications, such as mESC encapsulation in hydrogels for transplantation (Seo et al., 2023; Vuorenpää et al., 2024).

Gellan gum was also found to be extremely biodegradable and biocompatible. Gellan gum was used successfully in retinal engineering *in vivo* as endothelial cell sheet grafts with encouraging outcomes (Seo et al., 2023; Vuorenpää et al., 2024). The significant features of gellan gum which make it appropriate for tissue engineering are biocompatibility, endogenous similarity of glycosaminoglycans., nontoxicity, mild processing requirement, and mechanical behavior with close proximity to that of normal tissues (Palumbo et al., 2020; Wu et al., 2024). Da Silva et al. prepared gellan gum porous hydrogels with higher flexibility and enhanced mechanical strength. They employed these hydrogels to examine the biological reaction of stem cell differentiation in their three-dimensional matrix, which favored cell growth (da Silva et al., 2014). Additionally, Rim and colleagues created a cell delivery hydrogel system combining gelatin/gellan gum and gellan gum/glycol chitosan to facilitate the restoration of injured or diseased retinal tissue (Rim et al., 2020). Nevertheless, our

literature review reveals a lack of studies exploring the use of mESCs in conjunction with gellan gum.

Table 1***Biomaterials used in mESC culturing***

Types	Example	Properties	Reference
Natural polymer	Gellan gum	A structure like endogenous glycosaminoglycans, favorable mechanical characteristics like those present in native tissues and mild processing requirements.	(Lalebeigi et al., 2024; Osmałek et al., 2014)
	Silk fibroin	Materials derived from silk fibroin have been demonstrated to promote the growth of various ocular cell types.	(Adalı & Uncu, 2016; Ciocci et al., 2018)
	Sodium alginate	Alginate hydrogels have been extensively applied in stem cell cultures because of their biocompatibility, adjustable properties, high water content, improved mass transport characteristics, and ability to be functionalized with bioactive molecules to guide cell proliferation and differentiation.	(Rastogi & Kandasubramanian, 2019; Stachowiak et al., 2023)
	Collagen	Naturally found in the eye	(Na et al., 2021; Payne et al., 2017)

	Matrigel	Composed primarily of perlecan, laminin, entactin, and collagen type four, these components closely mimic the intricate microenvironment of the ECM.	(Sodunke et al., 2007)
	Hyaluronic Acid	Exhibits superior viscoelasticity, high moisture retention capacity, exceptional biocompatibility, and hygroscopic characteristics.	(Burdick & Prestwich, 2011)
Synthetic polymer	PLA, PLGA, PCL, PEG, PVA,	Facilitates straightforward modification, allowing for the design of specific properties.	(Kannan et al., 2022)

Silk fibroin has several advantages like facile fabricability into shapes, high tensile strength, high availability, biodegradability, transparency, and low immunogenic response (U.-J. Kim et al., 2004). Adalı & Uncu, (2016) cited that silk fibroin is non-thrombogenic, which further enhances its suitability for use in scenarios requiring enhanced hemocompatibility. Hang et al., (2021) cross-linked anisotropic hydrogels from silk protein nanofibers, which enhanced cell adhesion efficiently and were designed to replicate the physical milieu of the blastocoele. In the absence of leukemia inhibitory factors or mouse embryonic fibroblasts, hydrogels supported mESCs with stem cell characteristics *in vitro*. mESCs' growth on hydrogels led to increased pluripotency, genetic stability, developmental capacity, and effective germline transmission. These biomaterials were observed to support a more nurturing environment of change through autocrine factor secretion stimulation that supports and sustains embryonic stem cell proliferation.

2.3 Challenges the use of gellan gum

Because of biocompatibility, gellan gum is a very useful substance in tissue bioengineering and regenerative medicine, has the ability to form stable hydrogels, and encapsulates cells, so it is appropriate for cell encapsulation and tissue regeneration. However, there are several challenges that must be overcome to unlock its full potential (Palumbo et al., 2020).

Extensive characterisation of gellan gum and mixtures of other biomaterials must be carried out for their safety and biological compatibility (Mouser et al., 2016; Silva-Correia et al., 2011). Any variations and fluctuations in gellan gum formulation as well as differences in manufacturing steps may influence the cell and tissue interaction of its structure and consequently need standard testing procedures.

Improvement of the mechanical properties, including stiffness and elasticity, of the gellan gum scaffolds is required to obtain matching of the target tissue mechanical environment (Raghavendra et al., 2015). Additionally, regulation of the degradation rates of the scaffold for matching with the tissue healing process is required to obtain long-term functionality.

Strict tests need to be conducted to investigate how gellan gum scaffolds interact with cells and blood components. Testing for proliferation, adhesion of cells, proliferation, and differentiation on scaffolds and their impact on blood coagulation and immunological reaction is necessary in terms of forecasting their in vivo performance (Braune et al., 2013; Claudia Sperling et al., 2005; Weber et al., 2018).

Overcoming these challenges and looking ahead to future directions will enable us to gain a better understanding of the function of gellan gum in tissue engineering to broaden its applications in regenerative medicine. With the overcoming of these challenges, biomaterials derived from gellan gum can be potential key players in the development of new therapies for the treatment of many wounds and tissue diseases.

2.4.Hemocompatibility of biomaterials

For biomaterials in blood-contact devices, hemocompatibility is a key determinant of their clinical acceptability. ISO 10993-4 gives methods for the testing of the synergy interaction between blood components and biomaterials, including hemolysis, thrombogenicity, platelet activation, and tests of coagulation (Seyfert et al., 2002). It is especially important not to have a biomaterial to cause unwanted blood responses for use in vascular grafts, cell and drug delivery devices, wound dressings, and tissue engineering scaffolds. Hemocompatibility failure can also lead to life-changing and life-threatening complications such as thrombosis, immunodeviation, and inflammation reactions, whose intersection may make the material non-effective and unsafe (Moyo et al., 2023).

For biomaterials used in blood-contact devices, hemocompatibility is a major requirement for determining their clinical acceptability. ISO 10993-4 provides test methods for synergy interaction between biomaterials and blood components including hemolysis, thrombogenicity, platelet activation, and coagulation tests (Seyfert et al., 2002). It is particularly significant not to possess a biomaterial to elicit an undesired blood reaction for application in vascular grafts, drug and cell delivery devices, wound dressings, and tissue engineering scaffolds. Hemocompatibility failure can also produce life-altering and life-threatening complications including thrombosis, immunodeviation, and inflammation reactions whose intersection could render the material useless and risky (Moyo et al., 2023).

Blending sodium alginate with hydrogel matrices maintains the surface moist, a beneficial step in preventing excess blood coagulation and immune stimulation(Gao et al., 2022). The non-toxic gelation characteristic of sodium alginate also provides facile hydrogel surface creation, a feature that assists in platelet adhesion and response inhibition.

The synergistic integration of silk fibroin, gellan gum, and sodium alginate yields an improved blood-compatible composite biomaterial with minimized thrombotic risks through their synergistic effect (Moyo et al., 2024). These hybrid hydrogels have the optimal overall compromise between mechanical stability, swelling ability, and hemocompatibility and have widespread use in practically all fields of medicine, e.g., in cardiovascular tissue engineering and wound healing (Carrêlo et al., 2023; Lee et al., 2021; Moyo et al., 2024). Further research needs to entail the manipulation of their surface characteristics, their interactions with the constituents of blood over extended periods, and in vivo testing to establish their clinical relevance.

3. CHAPTER III Materials and methods

3.1 Materials

A purchase of the silk cocoons (*Bombyx mori*) was made at a local market in the Turkish Republic of Northern Cyprus. Sigma Aldrich was the procurement source for gellan gum and sodium alginate while the 3,500 molecular weight cut-off SnakeSkin® dialysis tubing was purchased from Thermo Fisher USA. EMSURE® Merck in Darmstadt, Germany is where Anhydrous sodium carbonate (Na_2CO_3), anhydrous calcium chloride (CaCl_2), and ethanol ($\text{C}_2\text{H}_5\text{OH}$) were sourced from. Sigma Aldrich supplied reagents for the swelling studies, including sodium acetate (CH_3COONa) Sodium phosphate monobasic (NaH_2PO_4), acetic acid (CH_3COOH), pH calibration buffers (pH 4, 7, & 10) and sodium phosphate dibasic (Na_2HPO_4). For the swelling using PBS, solid PBS capsules were provided by Sigma Aldrich. Additionally, Sigma Aldrich provided the MTT assay reagent MTT (3-(4,5-dimethylthiazol-2-yl)-2,5-diphenyltetrazolium bromide). For the LDH dehydrogenase assay the cytotoxicity assay kit was provided by Thermo Fisher Scientific. For the co-cultivation of mESC and STO cells, appropriate cell culture components were also utilized. Siemens Healthineers in Bavaria Germany supplied the reagents for the coagulation assays; Siemens Thromorel-S was used for Prothrombin Time (PT) analysis, Siemens Actin-FS was selected for Activated Partial Thromboplastin Time (aPTT) analysis, and Siemens Thromboplastin was utilized for fibrinogen assays.

3.2 Methods

3.2.1 Silk fibroin extraction and purification process

Silk cocoons were processed and arranged meticulously to produce a pure silk fibroin solution through a series of step-by-step processing steps, starting from washing the cocoons to remove dirt, impurities, and other contaminants.

3.2.1.1 Degumming process.

Degumming is also a crucial process in the process, whereby the sericin protein as an adhesive is removed from the silk cocoons. The process follows a procedure established by

Adalı and Uncu employing a thermochemical treatment. The process begins with the production of a sodium carbonate solution, by dissolving 12 grams of sodium carbonate in 200 mL of deionized water, and then mixing it with a magnetic stirrer to obtain homogeneity. Then, 2 grams of silk cocoons are added to a flask filled with the solution of sodium carbonate that has been prepared, and it is magnetically stirred for three hours. This is done three times by replacing the solution of sodium carbonate after every cycle. The silk cocoons are then washed properly with deionized water until the water is clear. Finally, the fibers are split with care and air-dried overnight (Adalı & Uncu, 2016).

3.2.1.2 Dissolution process.

Silk cocoons consist primarily of hydrophilic proteins known as sericin, which, in combination with fibroin, a water-insoluble protein, constitute around 70% of the cocoon composition. The gluey sericin is accountable for the degumming process. The degummed fibres thus obtained are dissolved in a concentrated electrolyte solution comprising 27.79 grams of CaCl_2 , 29.13 millilitres of ethanol ($\text{C}_2\text{H}_5\text{OH}$), and 36 millilitres of deionized water. This mixture is mixed continuously until the silk fibroin has completely dissolved, giving a concentrated solution of silk fibroin.

3.2.1.3 Dialysis.

To remove strong electrolyte molecules along with other contaminants from the silk fibroin solution, dialysis is used as a final step of purification. The solution is filled into a dialysis tube and that is placed inside a beaker containing deionized water. Deionized water is shaken at 90 rpm, and replaced every three hours to perform the purification. After the process is completed, the pure silk fibroin solution is suctioned from the dialysate using a syringe and poured into a vessel, as stipulated in the procedures.

3.2.2 Sodium alginate dissolution

For the purpose of preparing the solution of sodium alginate, 4.2% (w/v) was measured and added to the blend. It was stirred continuously at 100 rpm and heated to 60 °C. The solution was watched closely until the sodium alginate had dissolved and a good smooth and even blend was achieved.

3.2.3 Gellan gum dissolution

The gellan gum was accurately weighed and poured into a beaker, to be dissolved in distilled water. The four different concentrations were: 0.3%, 0.5%, 0.75%, and 1% (w/v). The gellan gum was dissolved by stirring on a magnetic plate at 90°C for 100 rpm for 2 hours until dissolution. Gently, calcium chloride was added to the solution at the concentration of 0.03% (w/v) and magnetically stirred for 10 minutes. Then the temperature was reduced to 60°C and stirring was maintained until a solution was homogeneous.

3.2.4 Hydrogel preparation

Gellan gum was used as the control biomaterial and prepared at four concentrations for two batches (m/V): 0.3%, 0.5%, 0.75%, and 1%, by the solution mixing method. Although the two batches were different in gellan gum concentration, the quantity and concentration of the other biomaterial were kept the same for both materials. Samples A-D were supplemented with 1.8 mL of 3% silk fibroin, while samples AA1-DA4 were supplemented with 4 mL of 4.2% alginate.

3.2.5 Swelling Kinetics

Swelling kinetics of hydrogel samples were investigated to proceed with the evaluation of their behavior and swelling properties. The aim was to determine the ratio of biomaterial swelling under controlled conditions. The hydrogel samples, each with a volume of 2 cm³, were tested with the assistance of a phosphate buffer solution in order to simulate the pH of the mESC microenvironment, as well as acidic body fluids. The eight hydrogel

samples were put in 156 for their swelling kinetics in acetate-buffered solution (ABS, pH 1.2) and phosphate-buffered solution (PBS, pH 7.4) both at 0.1 M. The dry weight (W_{dry}) of each hydrogel was measured and recorded before being placed in the warmed-up buffer solutions (37°C). After intervals of time, materials were, blotted on filter paper to remove excess surface fluid and then weighed immediately afterwards to obtain wet weight (W_{wet}). For swelling behavior calculation at particular times, the following formula was used:

$$\text{Swelling Ratio (\%)} = \left(\frac{\text{weight(wet)} - \text{weight(dry)}}{\text{weight(dry)}} \right) \times 100$$

This procedure permitted proper observation of the swelling behavior of the hydrogel and provided useful information regarding their potential use as a substrate for mESC's culturing.

3.2.6 Lyophilization

Eight individual hydrogels were lyophilized simultaneously at -60°C for 24 hours under a highly controlled process. Individual hydrogels were made and then put into balloon flasks, which were then put into protective containers. These were put into the lyophilization chamber of the Alpha 1-2 LSCbasic (Martin Christ) to achieve an even spread, thereby enabling uniform freezing and effective sublimation.

The samples were under slow cooling to -60°C in order to ensure complete freezing. The maintenance of this temperature for 24 hours enabled slow desiccation by sublimation. Pressure and temperature within the lyophilizer were controlled and monitored during this process to ensure optimal drying conditions.

After the cycle, new clean trays were utilized gradually to take out the freeze-dried hydrogels. Care was exercised while handling them so that they are not deforms or contaminated. This helped in freezing the eight hydrogels to dry their entirety without any loss of structure and properties.

3.2.7 Cell culture

The culturing of the cells was conducted in triplicate at Celal Bayar University. STO cell line (ECACC, Salisbury, UK), a fibroblast cell line routinely used as a feeder layer, was cultured in Dulbecco's Modified Eagle's Medium (DMEM) with 10% fetal bovine serum (FBS), supplemented with 1% L-glutamine and 1% penicillin/streptomycin for proper growth and viability of the cells. After reaching complete confluence in one week's time, STO cells were treated with a concentration of 20 µg/mL mitomycin-C (Applichem, Darmstadt, Germany) for 1.5 hours in standardized room conditions of 37°C and 5% CO₂, successfully inhibiting further cell division. After mitomycin-C exposure, the treated fibroblast cells served as a supportive layer for culturing embryonic stem cells (ESCs, CGR8, ECACC; Salisbury, UK). To ensure growth in its utmost capacity, an imperative medium DMEM with 4,500 mg/L glucose and sodium pyruvate (Biochrom AG, Berlin, Germany) to which 1% L-glutamine (Biochrom AG), 15% FBS (Biochrom AG), penicillin/streptomycin (1% Biochrom AG), 0.1 mM non-essential amino acids (Biochrom AG), and mercaptoethanol 10⁻⁶ M (Sigma-Aldrich, St. Louis, MO) were added. 1,000 IU/mL concentration of Leukemia inhibitory factor (LIF) (Sigma-Aldrich) was also added for self-renewal maintenance. For the control group, the medium used for ESCs cultured with STO cells was collected on days 1, 4, and 7 for further analysis. Concurrently, materials AA1, B, B-A-2, C, C-A-3, and D were conditioned for 24 hours with an ESC culture medium. Subsequently, the study groups were established by seeding ESCs cultured with STO cells onto the conditioned materials. The media from these study groups were collected on days 1, 4, and 7 for further analysis. Both control and study groups underwent cell viability assays and cytotoxicity tests. In this study, we used established mESC lines (CGR8, ECACC, Salisbury, UK) and mouse fibroblast (STO) cells (ECACC, Salisbury, UK). Since both cell lines are commercially available and previously established, ethical approval for their use is not required, and as such, no ethical approval is mentioned in this study.

3.2.8 Cell viability assay

To assess metabolic activity and membrane integrity, MTT and LDH assays were performed. ESCs co-cultured with STO fibroblasts were seeded into 96-well plates at a density of 2×10^3 cells/mL for the MTT assay, ensuring optimal conditions for viability evaluation. These cultures were incubated for 1, 4, and 7 days, and viability was assessed on each of these days for both control and experimental groups. A fresh MTT solution (2,5-diphenyl-2H-tetrazolium bromide) was prepared at a concentration of 5 mg/mL in PBS and passed through a filter to ensure purity before application. After incubation, an MTT solution was diluted 1:10 and dispensed into each well, followed by a 4-hour incubation at 37°C. To halt the reaction, 50 μ L of dimethyl sulfoxide (DMSO) was dispensed into each well. A microplate reader (ELX800UV, BioTek Instruments Inc) was used to measure absorbance at 540 nm. The LDH cytotoxicity assay assesses cell membrane damage by quantifying LDH activity in the surrounding medium. The Diaphorase reaction forms the basis of this assay, where LDH facilitates the conversion of lactate to pyruvate, simultaneously reducing NAD⁺ to NADH and releasing H⁺. After obtaining the generated NADH/H⁺, the yellow tetrazolium salt INT is reduced, resulting in the formation of a red formazan product. The amount of formazan formed, proportional to LDH activity, increases with the number of dead or membrane-damaged cells. The controls consisted of ES culture medium without cells, ES culture medium with cells, and ES culture medium with cells treated with Triton X-100. A volume of 50 μ L of supernatant was transferred to the corresponding wells of a 96-well plate, followed by the addition of 50 μ L of the reaction mixture. The plate was incubated in the dark at 15-25°C for a duration of 30 minutes. Absorbance was then measured at 490 nm. LDH activity was calculated according to the protocol provided with the LDH assay kit (Celltechgen CTG-CT0001).

3.2.9 Differential scanning calorimetry (DSC)

Thermal analysis was carried out at Middle East Technical University (METU). Amongst all hydrogel biomaterial lyophilized samples, four of them were selected and analyzed using the DSC250 machine to find out the peak point temperatures before

degrading. Nitrogen gas provided a constant condition via major parameters 10°C/minute, from 25°C to 180°C. This enabled the assessment

of how the hydrogels reacted to the change in temperature throughout the whole range. These and the maximum temperatures, phase changes, and at what phase the material starts to deteriorate tell us about hydrogels' behavior with regard to response to change in temperature, a matter of concern with regard to application where stable material is needed.

Overall, using the DSC250 with nitrogen allowed us to fully analyze the response of the hydrogels to heating and provided useful data for moving forward with the refinement of the material and study.

3.2.10 Scanning electron microscopy (SEM)

Surface morphology characterization of lyophilized hydrogels was performed on a Thermo Scientific Apreo S SEM at Middle East Technical University (METU). Charging was prevented by sputter coating the samples with a 7 nm thick gold-palladium (Au/Pd) alloy layer. Secondary-electron in-lens mode SEM imaging, optimized for high-magnification zoom, was used. The accelerating voltage of the microscope was 5 kV, and the working distance was 10 mm. The samples were imaged at 100 μ M magnification to allow for high-resolution morphological examination of the biomaterials. The images were processed using EDAX Genesis software to estimate pore size and distribution by measuring from at least three different regions of each sample for statistical significance. SEM instrument calibration was conducted before each imaging session using a reference material in a standard form to ensure accuracy and consistency.

3.2.11 Blood biocompatibility

Donor blood was donated and segregated into sodium citrate (Na citrate) and dipotassium ethylenediaminetetraacetic acid (K₂EDTA) tubes for experiments in Figure 2. Untreated blood was placed in blank tubes, negative controls were shaken and incubated, and following centrifugation of Na citrate tubes at 850 rpm for 10 minutes, plasma was analyzed for PT, aPTT, and fibrinogen levels. After incubation of the hydrogel-treated

samples at 37°C for 1 hour, PT, aPTT, and fibrinogen were assessed, while CBC, hemolysis studies, and peripheral blood smears were performed in K2EDTA tubes. The hydrogel-contacted blood was used to prepare smears, which were stained and assessed for platelet adhesion and erythrocyte morphology under 400× magnification, while the hemolysis index was measured by centrifuging the K2EDTA tubes at 850 RPM for 10 minutes.

Treated whole blood was magnetically spun at 100 rpm for 1 hour, then centrifuged, and hemolysis index was measured in the plasma. This was carried out to ascertain that the likely hemolytic action of the hydrogel treatment could be effectively assessed.

These were conducted to thoroughly test the interaction between the hydrogel and blood components. PT, aPTT, and fibrinogen tests were used for coagulation pathway analysis, and the CBC and hemolysis analysis provided information on the impact of the hydrogel on red blood cells and general blood conditions. Erythrocyte morphology and platelet adhesion analysis through peripheral blood smears was critical in evaluating the biocompatibility of the hydrogel.

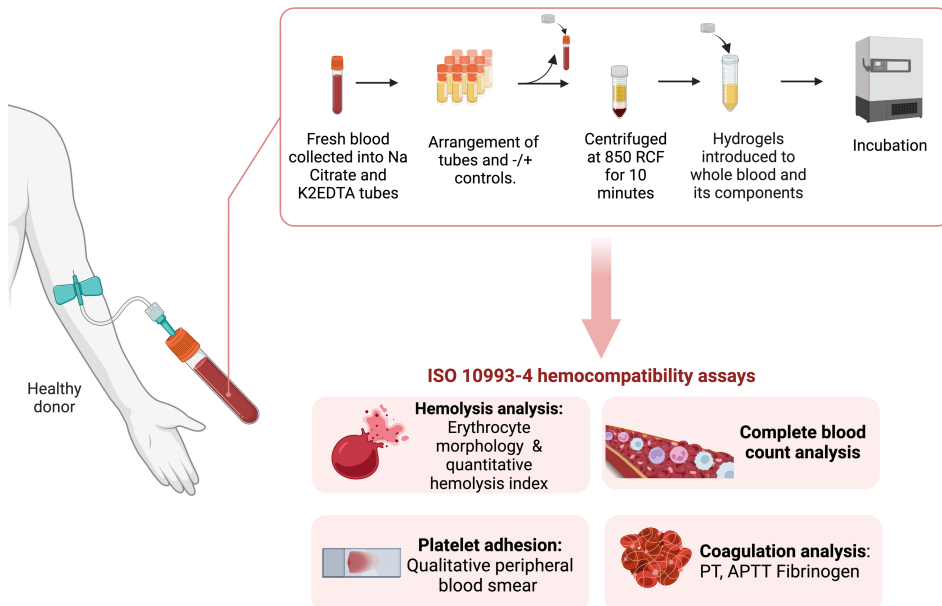


Figure 2

ISO 10993-4 hemocompatibility assay steps

3.2.11.1 In-vitro clotting assessment

Coagulation parameters, including PT, aPTT, and fibrinogen levels, were measured using the Sysmex CS-1600 Automated Coagulation Analyzer with Siemens reagents, with results reported in seconds for PT and aPTT. Fibrinogen levels were reported in mg/dL.

3.2.11.2 Complete blood count profile.

Using the Sysmex XN-1000 Automated Hematology Analyzer, the primary hematological parameters were analyzed, including red blood cell (RBC) count, mean corpuscular hemoglobin concentration (MCHC), hemoglobin concentration, white blood cell (WBC) count with differential, platelet count, and indices such as mean corpuscular volume (MCV). The analyzer was calibrated and quality controls were run before experimenting in order to achieve precise and dependable results. The interpretation of complete blood count (CBC) results was completed by utilizing reference ranges, through which any potential hydrogel effects on blood components could be determined.

3.2.11.3 Hemolysis quantification index.

With the Abbott Architect C4000 Automated Biochemistry Analyzer, the hemolysis index was tested by detecting the degree of hemolysis of samples in order to evaluate the effects of hydrogels on the stability of blood cells and corresponding biochemical indices.

3.2.11.4 Analysis of erythrocyte structure and platelet adhesion.

Blood and hydrogel were combined in test tubes and shaken at 150 rpm for 45 minutes at room temperature using an IKA KS 260 shaker, followed by incubation at 37°C for 1 hour. Peripheral blood smears were prepared, air-dried, and alcohol-fixed, and stained using the Wright-Giemsa method. The platelet adhesion and erythrocyte morphology were then qualitatively assessed to identify the occurrence of any shape defects in erythrocytes

and to track interactions of platelets with the hydrogel matrix. The stained smears were observed under a microscope at 450 μm magnification, and the analysis was performed over 10 different fields.

4. CHAPTER IV

Findings and discussion

4.1 Formulations of hydrogels

Outlined Listed in Table 2 are the individual formulations to facilitate extensive analysis of the possible application of hydrogels in biomedical fields. The individual samples were subjected to harsh testing regimens to obtain data on thermal stability, swelling ability, coagulation behavior, hemolysis ability, and blood cell compatibility. These extensive studies informed us regarding the functionality and the degree to which gellan gum hydrogels operate, and the possibility of utilizing them for various clinical and research-oriented applications.

Table 2

Formulated hydrogels and their compositions

Sample	Gellan gum concentration (%)	Silk fibroin concentration (%)	Sodium alginate concentration (%)
A	0.3%	3%	-
B	0.5%	3%	-
C	0.75%	3%	-
D	1%	3%	-
AA1	0.3%	-	4.2%
BA2	0.5%	-	4.2%
CA3	0.75%	-	4.2%
DA4	1%	-	4.2%

4.2 Swelling kinetics.

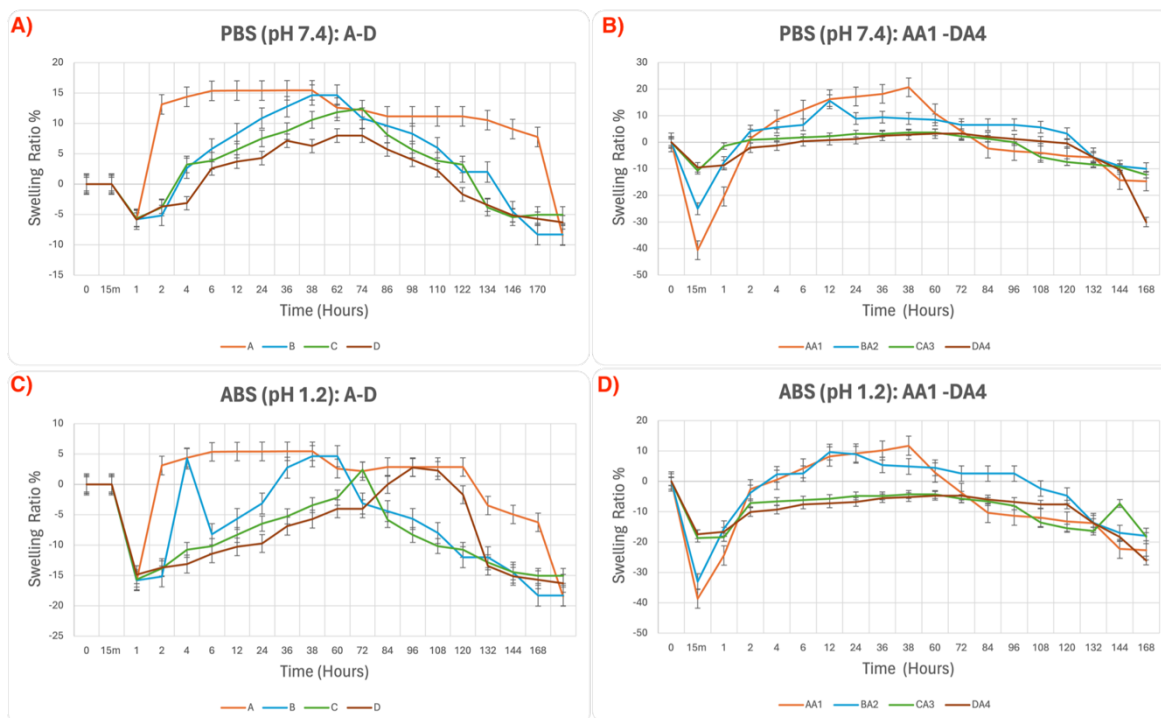


Figure 3

Gellan gum hydrogel swelling in PBS (A, B) and ABS (C, D).

We observed in our research that hydrogels swelled to a higher swelling ratio in PBS compared to ABS. This may be attributed to the buffering capability and pH differences between ABS (pH 1.2) and PBS (pH 7.4), whereby PBS's increased pH enables more swelling due to greater ionization and electrostatic repulsion of the hydrogel network. Besides, as revealed in Figure 3, our findings identified appreciable differences among hydrogels treated with sodium alginate and silk fibroin. The hydrogels with silk fibroin had better stability and lower swelling ratios compared to the hydrogels with sodium alginate. The finding implies that silk fibroin might create denser crosslinking of the hydrogel matrix, thus reducing water absorption and enhancing strength. We also investigated the impact of gellan gum concentration on hydrogel swelling behavior. Our results repeatedly indicated that increased gellan gum concentrations resulted in decreased swelling capacity. This phenomenon is most probably due to increased crosslinking density and reduced pore size

in the hydrogel network, limiting the absorption and storage of water within the structure. In summary, our findings identify the contributions of buffer composition, biomaterial choice (silk fibroin vs sodium alginate), and effect of polymer concentration on hydrogel swelling response. These findings are pivotal in the optimization of hydrogel product design and performance in biomedical and therapeutic applications.

4.3 Cell culture.

The fibroblastic morphology of STO cells and mESCs was systematically explored in all the hydrogel samples. Upon analysis of cultures, it was noted that the STO cells preserved their unique fibroblastic morphology, as seen from Figures 4A and 4B. Remarkably, this morphology was preserved even upon treatment with mitomycin C, as shown in Figure 4 C and D. Following treatment of confluent STO cells with mitomycin C, the mESCs were observed to be rounded in shape with distinctively bright nuclei, as in Figure 5. The mESCs went on to further develop by adhering together in the culture plates, ultimately forming well-established colonies that were distinctively observable from the remainder of the mouse fibroblast cells, as in Figure 5.

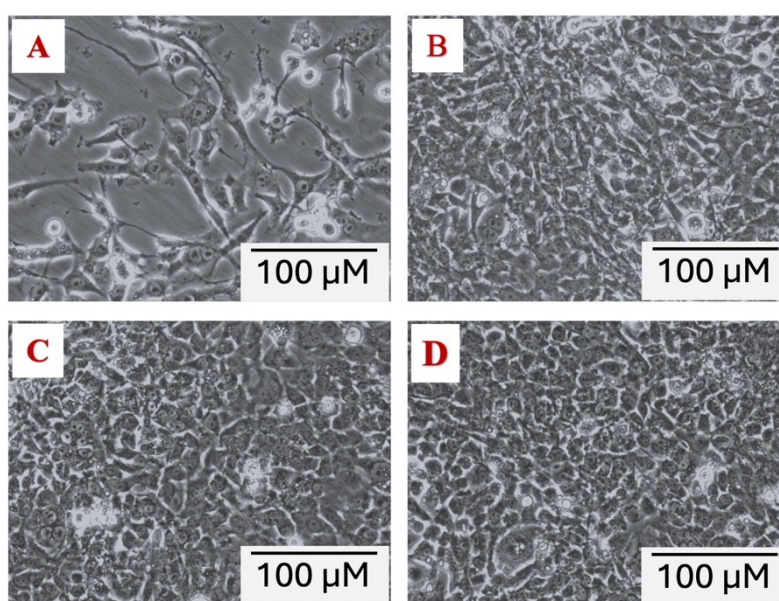


Figure 4
Morphological changes in STO cells during culture.

(A) STO cells at day 3 of culture and (B) STO cells at day 5 of culture. (C, D) STO cells after Mitomycin-C administration. Scale bar: 100 μm .

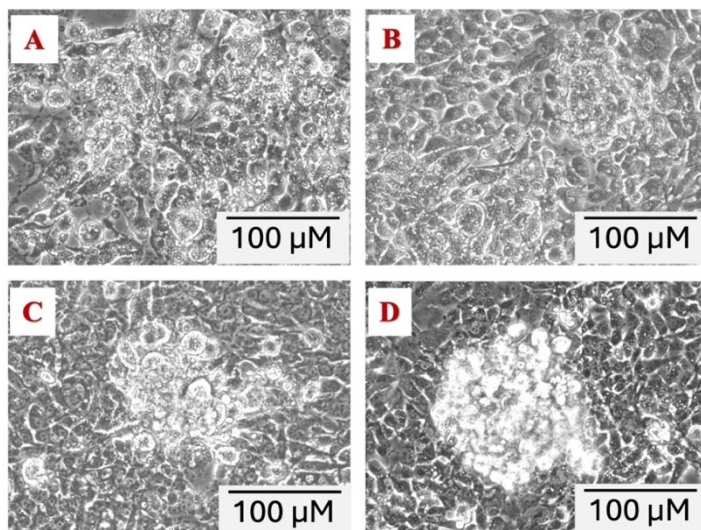


Figure 5

Images of STO + mESC co-culture over time.

(A–D) Representative images of STO + mESC co-cultures at (A) Day 0, (B) Day 1, (C) Day 4, and (D) Day 7. show progressive changes in colony morphology. At first, individual mESCs were rounded with well-defined, bright nuclei on the mitomycin C-treated STO feeder layer. Over time, mESCs became attached to one another and developed compact colonies that became increasingly demarcated from the overlying fibroblast layer. By Day 4, small clusters had grown into large, dense colonies, which continued to grow in size and number by Day 7. General colony growth in size and number is a sign of healthy proliferation and self-renewal of mESCs in the co-culture system. Scale Bar: 100 μm

The mESCs cultured with STO on various materials also demonstrated obvious differences in colony formation. Fewer colonies developed on AA1 and CA3, with a visible reduction in number with time (Figure 6A, E; 7A, E; and 8A, E). This loss may be due to suboptimal material properties, which may adversely affect cell adhesion, limit nutrient diffusion, or induce stress that inhibits proliferation. For materials B and D, whilst well-formed colonies were seen in the first day, colony growth declined in advanced stages of culture (Figure 6B, F, Figure 7B, F, and Figure 8B, F), maybe due to accumulated cellular stress or

differentiation-associated effects. Conversely, BA2 and C materials had a support of increased numbers of colonies in subsequent stages (Figure 6C, D; 7C, D; and 8C, D), suggesting that such materials provided an improved microenvironment for long-term mESC proliferation. Control cells also presented stable colonies on Day 1, Day 4, and Day 7, reflecting normal proliferation under standard conditions (Figure 6G, Figure 7G, and Figure 8G). Lower colony number over time on certain materials suggests that material properties and prolonged culture conditions are significant determinants of the survival and growth of mESCs.

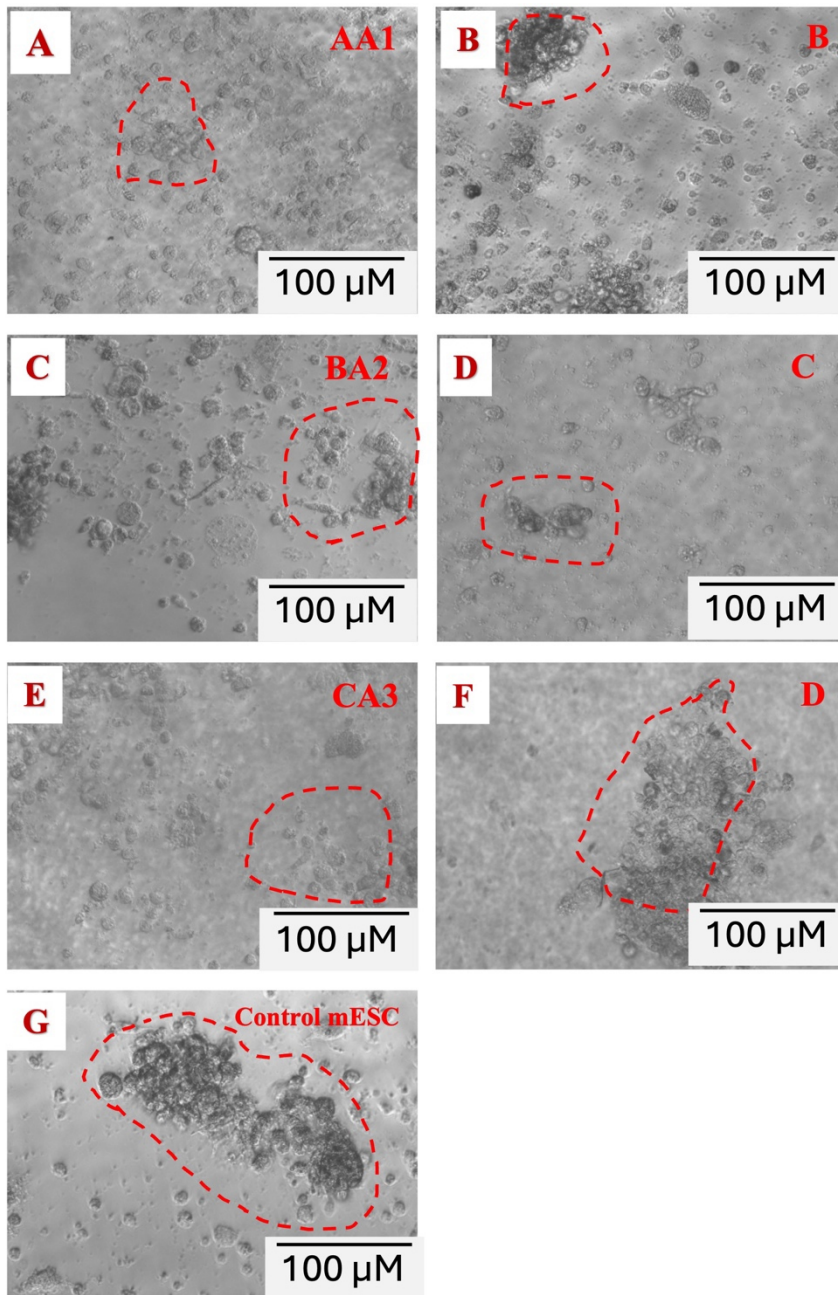


Figure 6
Morphology of mESCs with hydrogels on day 1

Control mESCs cultured in the absence of hydrogel materials, as a control for comparison purposes. Day 1 Photo of mESC cultured with material AA1 (A), B (B), BA2 (C), C (D), CA3 (E), and D (F). Control mESC (G). Scale Bars: 100 μM . Distinct differences in cell attachment, spreading, and colony formation are apparent with the different hydrogel conditions.

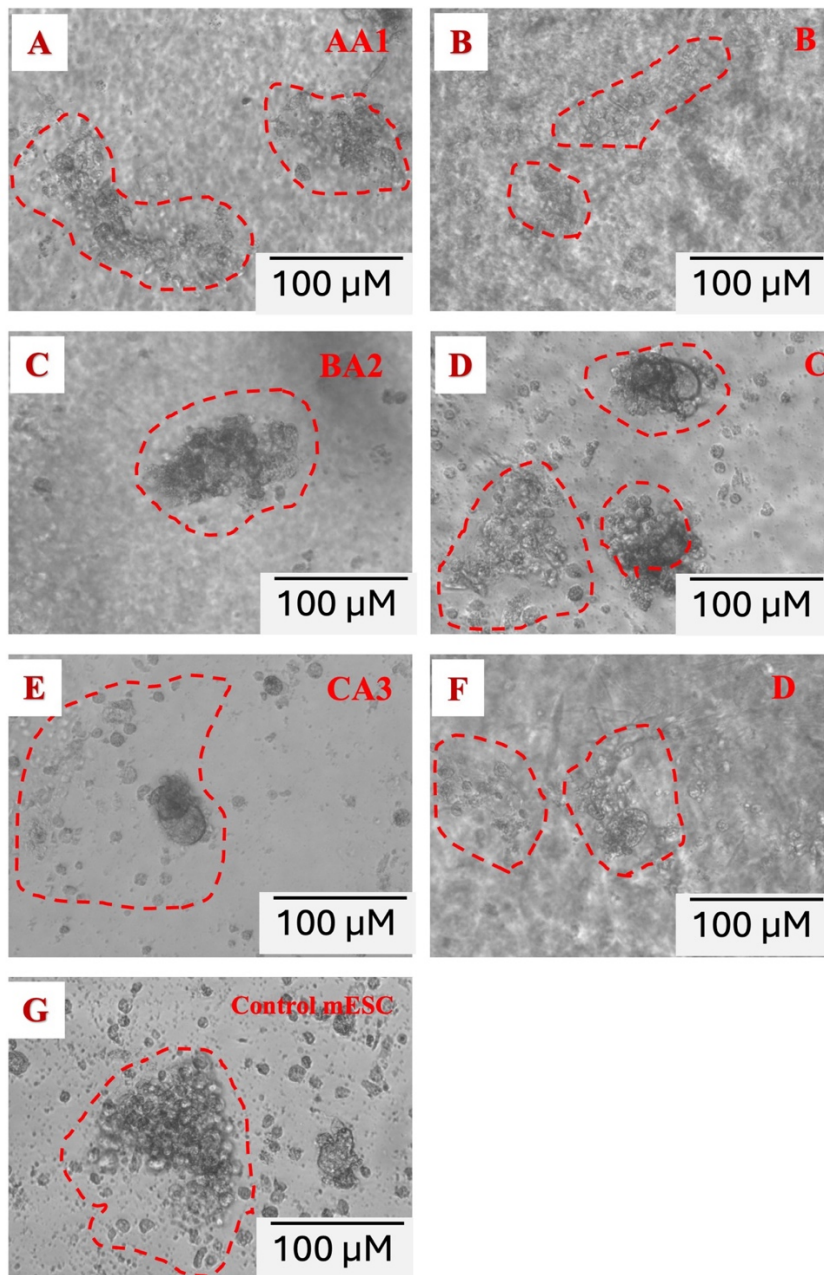


Figure 7
Morphology of mESCs with hydrogels on day 4.

Representative microscopic images illustrate morphology of mESCs cultured in various hydrogel preparations at Day 4. Microscopic picture of mESC Cultured using materials AA1 (A), B (B), BA2 (C), C (D), CA3 (E), And D (F). Control mESC (G). Scale Bars: 100 μm.

Distinct differences in morphology and cell aggregating behavior are observed with different composition of hydrogels. mESCs in sodium alginate containing gels (A,C,E) express some form of clustering, suggesting certain distinct interactions with the substrate. The mESCs in silk fibroin containing hydrogels (B, D, F) have dispersed or attached-like morphology, which may reflect better surface interactions and biocompatibility of the material with the cell. The control group (G) serves as a reference, and it displays normal undifferentiated mESC morphology in the normal culture conditions. These results provide information regarding the impact of hydrogel composition on attachment, proliferation of stem cells, and overall cell behavior.

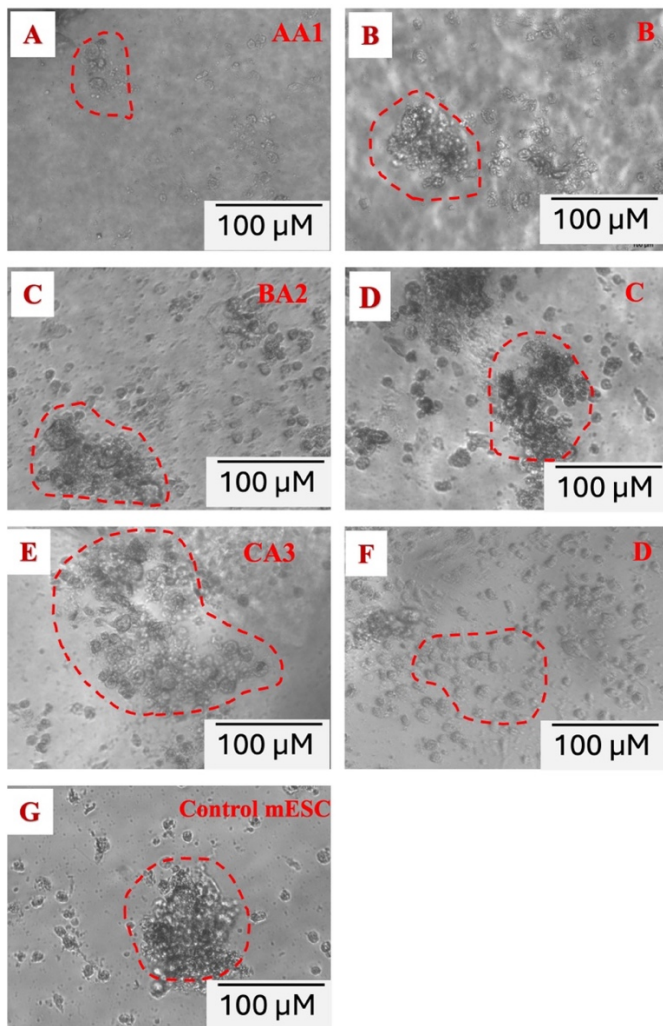


Figure 8

Morphology of mESCs with hydrogels on day 7.

Representative microscopic images demonstrate the morphology of mESCs cultured on various hydrogel formulations after seven days of incubation. Images are for mESCs cultured on AA1 (A), B (B), BA2 (C), C (D), CA3 (E), and D (F), with control mESCs cultured on a standard substrate in (G). Scale bars represent 100 μm .

By Day 7, differences in cell morphology, aggregation, and distribution patterns are evident among the different hydrogel compositions. mESCs on AA1 (A), BA2 (C), and CA3 (E) exhibit dense, rounded colonies characteristic of strong cell-cell adhesion and potential maintenance of pluripotency. Cells on hydrogels B (B), C (D), and D (F) exhibit more spread morphologies, potentially indicative of altered cell-material interactions and potentially increased adhesion to the substrate.

Control group (G) displays normal undifferentiated mESC morphology, serving as a reference for normal colony formation under routine culture conditions. The results emphasize the role of hydrogel composition on stem cell attachment, proliferation, and self-renewal over extended durations.

4.4 MTT results

Used to quantify cell viability and proliferation, the MTT assay is a colorimetric assay that quantitates the reduction of MTT to a purple formazan product by living cells. The amount of formazan produced is directly proportional to the number of living cells and can be used to determine metabolic activity and the effect of different treatments or conditions.

mESCs were co-cultured with STO cells on materials AA1, B, BA2, C, CA3, and D for 1, 4, and 7 days, as indicated in Figure 9. MTT assay was employed to measure cell viability and examine cell proliferation kinetics over the culture duration. All of the materials had comparable viability to promote ES cell growth on day 1. Nonetheless, by day 4, significant differences in cell viability were evident between the different groups. Specifically, materials AA1, B, C, and D exhibited a severe reduction in cell viability compared to BA2 and CA3,

reflecting their variation in supporting cell growth throughout the period. By day 7, further differences in cell viability were apparent. Materials C and CA3 performed better with higher cell viability compared to the other test materials. This indicates that materials C and CA3 can create a more suitable condition for long-term cell survival and proliferation compared to materials AA1, B, BA2, and D.

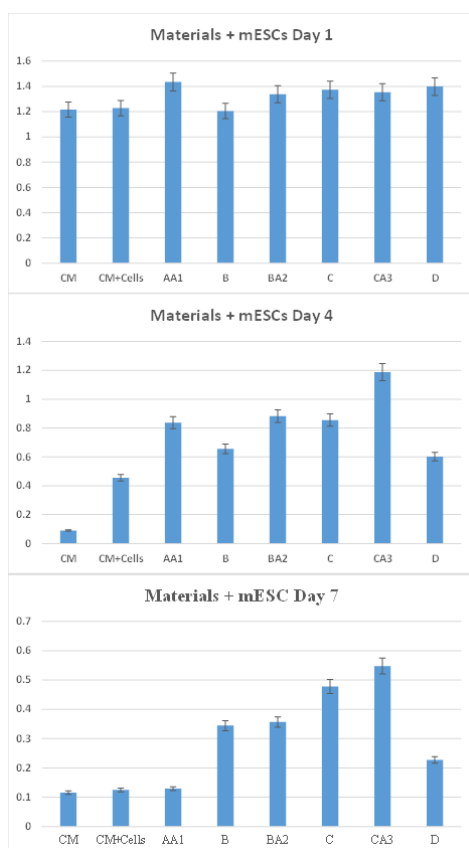


Figure 9

MTT Results for day 1, 4 and 7 of mESC ,CM and hydrogels.

In CM, cell viability was assessed using the MTT assay on day 1, 4, and 7, culture medium with STO cells (CM+Cells), and biomaterials (AA1, B, BA2, C, CA3, and D). Cell viability on day 1 was alike in all the conditions. On day 4, viability was reduced considerably in AA1, B, BA2, and D compared to BA2 and CA3. AA1 and B showed a drastic reduction in viability between days 4 and 7. The reduction was so pronounced that it could be due to material degradation within this time period, which could have compromised hydrogel mechanical stability or released cytotoxic byproducts. Byproducts could interfere with cell

processes, leading to reduced viability. Additionally, changes in nutrient diffusion, mechanical property changes of the biomaterials, or perturbed cell-matrix interactions may also have caused decreased cell adhesion and proliferation. On the contrary, by day 7, C and CA3 showed improved viability, suggesting that these materials were more stable or supportive as a microenvironment for mESC development. LDH assay data presented in Figure 10 also illustrated material-dependent differences in cell proliferation and cytotoxicity. These findings were reproducible in three independent experiments, demonstrating the reliability of the results.

4.5. Lactate dehydrogenase cytotoxicity detection

To assess cell membrane integrity, the LDH assay measures leakage of LDH into culture medium upon damage or disruption of cells. The level of LDH in the medium is directly proportional to the degree of cellular damage or cytotoxicity. It is commonly used to assess cell viability and the extent of cellular injury or death.

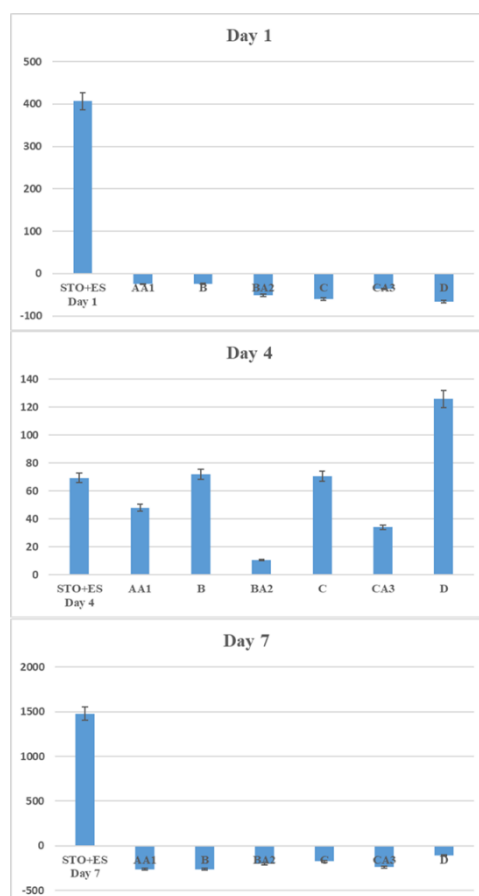


Figure 10

LDH results for day 1, 4 and 7 of mESC ,CM and hydrogels.

Figure 10 shows the LDH assay data comparing cytotoxic activity of different biomaterials (AA1, B, BA2, C, CA3, and D) against mESCs co-cultured with STO cells for seven days. On day one, all biomaterials tested were shown to be of low cytotoxicity, which means cell viability was relatively uninhibited. On day four, however, cytotoxicity was heightened in AA1, B, and C, while D evidenced maximum LDH release indicating major cell destruction. BA2 and CA3 evidenced quite minimal cytotoxicity. By day seven, however, cytotoxicity was down in all the biomaterials as indicated by minimum LDH release, indicative of the fact that no further cell destruction was occurring. These findings substantiate that cytotoxic effects are time-dependent and vary with the composition of biomaterial employed.

4.6 Differential scanning calorimetry(DSC)

DSC is a technique to measure the heat flow of phase transitions in materials, i.e., melting, crystallization, or glass transition. Heating or cooling a sample and comparing the heat flow to a reference, DSC provides information on the thermal properties, stability, and composition of the material. This can be particularly useful to examine biomaterials, polymers, or hydrogels.

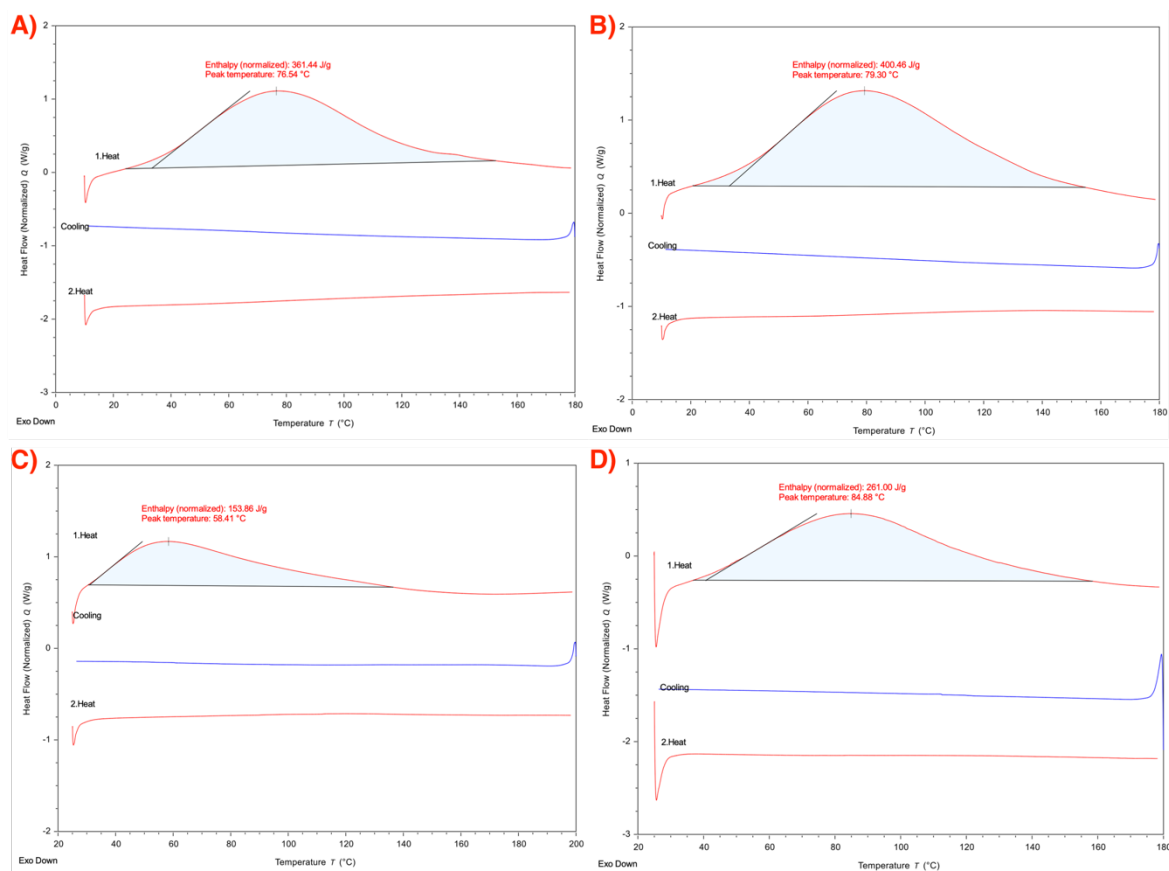


Figure 11
DSC thermograms

Figure 11 showing the thermal transitions of four scaffolds: (A) BA2, (B) DA4, (C) C, and (D) D. Each curve represents heat flow as a function of temperature in a nitrogen environment, spanning from 25°C to 180°C with a heating rate of 10°C/min.

4.7 Scanning electron microscopy (SEM)

By focusing a narrow electron beam on the surface of a sample, SEM generates signals from electron interactions with the atoms of the target material. These signals form detailed images of the structure, shape, and chemical composition of the surface. It is primarily employed to study materials' microstructure at the microscopic level, such as biomaterials and cells.

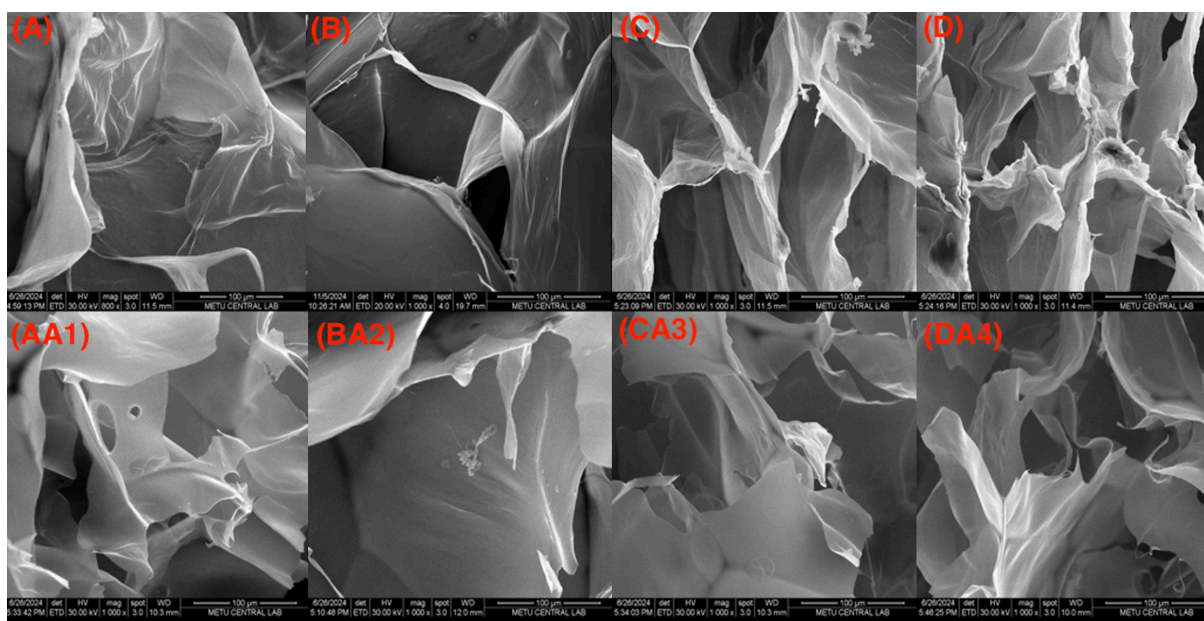


Figure 12
SEM images

Figure 1 presents a morphological analysis at 100 μm magnification, illustrating the surface characteristics of gellan gum-based hydrogels and highlighting distinct structural differences between the silk fibroin (A–D) and sodium alginate (AA1–DA4) formulations, revealing notable variations in their surface structures.

4.5 Hemocompatibility studies.

Surface characteristics, such as roughness, topography, and texture, are significant in regulating the hemocompatibility of gellan gum-based hydrogels. Such physical characteristics are relevant to the regulation of how the hydrogels interact with the various constituents of blood, as confirmed by hemocompatibility assay results. Specifically, smoother surfaces were revealed to minimize undesired interactions with both plasma proteins and blood cells, lowering the activation of coagulation cascade and hemolysis. Conversely, rougher or more irregular surfaces can promote platelet adhesion and aggregation and thus induce thrombotic responses. The analysis of erythrocyte morphology also illustrates the influence of surface characteristics, as hydrogels with optimized surfaces maintained the structural integrity of red blood cells with no deformation or lysis. The findings collectively indicate that the alteration of surface characteristics of gellan gum-based hydrogels is important in improving their hemocompatibility, with profound effect on their potential use in blood-contacting applications such as drug delivery systems, vascular grafts, and wound dressings.

4.5.1 Complete blood count assessment

Table 3 shows CBC values for hydrogel-treated specimens, negative control and blank. All significant parameters were within clinically acceptable values, showing no unwanted effects on the blood components by the hydrogels. Specifically, the red blood cell (RBC) counts were between 5.35 and $5.60 \times 10^6/\mu\text{L}$, and the white blood cell (WBC) counts were between 4.00 and $4.93 \times 10^3/\mu\text{L}$. Platelet counts were also consistent in all the groups between 337 and $365 \times 10^3/\mu\text{L}$ without deviation, and hemoglobin (HGB) was also consistent at 16.2 to 16.4 g/dL. In addition, the mean corpuscular volume (MCV) and mean corpuscular hemoglobin (MCH) values indicated no abnormal changes, ensuring function and morphology of blood cells were maintained. Absence of abnormal blood reactions, such as hemolysis or platelet activation, emphasizes the hemocompatibility of the hydrogels. These findings collectively ensure the hydrogels are nontoxic and well tolerated and

therefore appropriate for blood-contact applications, attesting to their desirable utility in biomedical therapies and devices.

Table 3***Complete blood count (CBC) assessment***

Blood cells	Measurement units	Standard range	Blank sample	Negative control	A	B	C	D	AA1	BA2	CA3	DA4
White blood cells (WBC)	[10 ³ /μL]	4.0–11.0	5.21	5.9	4.64	4.75	4.67	4.93	4.67	4.73	4.40	4.44
Red blood cells (RBC)	[10 ⁶ /μL]	4.2–6.1	5.67	5.59	5.41	5.42	5.52	5.42	5.35	5.44	5.38	5.60
Hemoglobin (HGB)	[g/dL]	12.1–17.2	16.8	16.5	16.3	16.4	16.4	16.3	16.3	16.4	16.2	16.4
Hematocrit (HCT)	[%]	36–54	48.6	48.1	46.7	46.8	47.5	46.9	46.2	46.8	46.4	48.3
Mean corpuscular volume (MCV)	[fL]	80–100	85.9	86.1	86.5	86.5	86.2	86.7	86.5	86.2	86.4	86.2
Mean corpuscular hemoglobin (MCH)	[pg]	27–33	29.6	29.6	30.1	30.2	29.7	30.0	30.4	29.9	29.7	29.6
Mean corpuscular hemoglobin concentration (MCHC)	[g/dL]	31.5–35.5	34.5	34.4	34.8	35.0	34.4	34.7	35.2	34.7	34.7	34.1
Platelets (PLT)	[10 ³ /μL]	150–450	365	361	340	337	350	350	338	359	365	340

Red cell distribution												
width-standard deviation (RDW-SD)	[fL]	35–55	40.3	40.2	41.0	40.4	40.3	41.2	40.8	40.8	40.7	40.5
Red cell distribution												
width-coefficient of variation (RDW -CV)	[%]	11.5–14.5	12.9	12.7	13.4	13.2	13.0	13.3	13.3	13.3	13.0	13.3
Platelet distribution												
width (PDW)	[fL]	9–17	10.7	10.6	10.6	10.7	11.2	11.3	11.6	10.7	10.9	10.2
Mean platelet volume (MPV)												
	[fL]	7.5–11.5	9.6	9.7	9.7	10.0	10.0	9.9	9.8	10.3	9.9	9.9
Platelet-large cell ratio (P-LCR)												
	[%]	15–30	20.8	23.1	21.4	23.0	22.9	23.0	21.8	24.3	23.3	21.6
Plateletcrit (PCT)												
	[%]	0.2–0.5	0.36	0.34	0.34	0.35	0.36	0.36	0.34	0.38	0.36	0.35
Nucleated red blood cells (NRBCs)												
	[10 ³ /μL]	0–2	0.00	0.00	0.00	0.00	0.00	0.00	0.00	0.00	0.00	0.00
Neutrophils (Neut)												
	[10 ³ /μL]	1.8–7.8	2.66	2.70	2.42	2.69	2.61	2.55	2.70	2.53	2.29	2.36
lymphocytes (Lymph)												
	[10 ³ /μL]	1.0–4.8	2.05	1.86	1.73	1.75	1.74	1.62	1.66	1.73	1.64	1.63
Monocytes (Mono)												
	[10 ³ /μL]	0.2–0.8	0.46	0.38	0.42	0.43	0.43	0.47	0.40	0.41	0.39	0.38
Eosinophils (Eo)												
	[10 ³ /μL]	0–6	0.08	0.06	0.08	0.09	0.09	0.10	0.08	0.08	0.08	0.07
Basophils (Ba)												
	[10 ³ /μL]	0–0.2	0.02	0.01	0.02	0.02	0.02	0.03	0.03	0.02	0.02	0.02

Immature granulocytes (IG)	[10 ³ /μL]	0.0–0.1	0.01	0.01	0.01	0.02	0.02	0.02	0.01	0.02	0.01	0.01
-------------------------------	-----------------------	---------	------	------	------	------	------	------	------	------	------	------

4.5.2 Coagulation analysis

Coagulation analysis of test samples was compared to control samples. Table 4 shows that the fibrinogen, PT, and aPTT levels of all test samples were within normal ranges. This is direct evidence that test samples did not influence coagulation parameters, hence providing a hemostatic balance similar to that of control samples.

Table 4

Coagulation analysis of test samples against controls

Parameter	Standard range	Blank	Negative control	A	B	C	D	AA1	BA2	BA3	BA4
PT (Sec)	10–14	12.2	12.7	12.3	12.5	12.6	12.8	12.5	12.7	12.8	13.1
aPTT (Sec)	25–35	28.2	25.0	27.3	27.0	27.7	28.2	28.3	28.5	29.8	30.7
Fibrinogen (mg/dL)	200–400	200.9	172.9	203.3	200.6	206.1	206.1	195.4	195.4	195.4	192.9

Table 4 presents the hydrogel sample coagulation parameters, negative control, and blank. Fibrinogen level was marginally less than normal (200–400 mg/dL) in all of the sodium alginate-treated groups, with the maximum decrease observed in the sodium BA4 group. The fibrinogen level was, however, sufficient to cause clot formation without any serious inhibition.

Values for PT ranged from 12.3 to 13.1 seconds, and those for aPTT ranged from 27.0 to 30.7 seconds. All the values were within clinical normal ranges, indicating that there was no significant effect of the hydrogels on coagulation pathways.

In comparison of the hydrogel preparations, the silk fibroin-derived hydrogels (A-D) had marginally increased clotting times, indicating speeded-up activation of the extrinsic coagulation pathway. Alternatively, sodium alginate-derived hydrogels (AA1-DA4) had increased clotting times, suggesting altered coagulation profiles, indicating reduced initiation of the intrinsic pathway of coagulation.

These findings highlight the role of hydrogel composition in blood coagulation kinetics. Silk fibroin hydrogels enabled speeded clotting, but sodium alginate hydrogels extended clotting time and impacted fibrinogen level, which was reduced minimally. These findings highlight

material-dependent interactions with blood components and provide important insights into hydrogel hemocompatibility for medical use. Supplemental CBC analyses corroborate these findings.

4.5.3 Quantitative hemolysis index analysis

As shown in Table 5, quantitative analysis indicated a minor level of hemolysis in all test samples, while hemocompatibility remained within acceptable limits.

Table 5

Quantitative hemolysis index analysis

Parameter	Standard Range	Blank	Negative Control	A	B	C	D	AA1	BA2	CA3	DA4
Hemolysis index	30/0	25/0	23/0	46.4/1+	56.5/1+	59.2/1+	66.4/1+	22.9/0	39.0/1+	40/1+	39.5/1+

Table 5 illustrates variation in hemolysis of hydrogel samples with surface properties during RBC lysis. Sample A of gellan gum–silk fibroin hydrogels revealed a hemolysis index of 46.4/1+, while sample D reached 66.4/1+, since hemolysis was promoted by higher gellan gum contents. AA1 revealed lowest hemolysis (22.9/0), reflecting good compatibility with blood cells. Normal hemolysis was encountered in the 0.5% and 0.75% gellan gum formulations, whereas those of 1% gellan gum induced greater RBC lysis, though not to an excessive degree. Hemolysis indices of BA2 and CA3 were 39.0/1+ and 40/1+, respectively, still within the acceptable blood-contact material limit. Further increasing to 1% gellan gum led to greater hemolysis, as encountered for the DA4 formulation. While increased gellan gum concentrations produced greater hemolysis, the net effect was still within a moderate level, which suggests that the formulations were still acceptable for biomedical uses. Since hemolysis index <30/0 is typically taken as a critical test of hemocompatibility, the following results indicate that despite the elevated level of gellan gum that tends to raise hemolysis, the net effect is low and confirms the feasibility of using such hydrogels in blood-contacting applications.

4.5.4 Erythrocyte structural analysis and platelet adhesion assessment.

Figure 13 presents peripheral blood smear tests and erythrocyte morphology studies, which play a vital role in determining the hemocompatibility of 400 μm hydrogels. Hydrogels containing 0.3% and 0.5% gellan gum (A, B) revealed no significant changes in RBC morphology or platelet aggregation, suggesting that these concentrations neither induce RBC damage nor platelet adhesion. On the other hand, 0.75% gellan gum hydrogels (C) presented minimal hemolysis and a marginally denser yet still normal platelet distribution, indicating very little effect on erythrocytes and platelets. Hydrogels with the highest gellan gum concentration (D and DA4) exhibited dispersed dysmorphic erythrocytes and partial platelet clumping, most likely due to surface roughness. On the other hand, more smooth surfaces—such as in A, B, AA1, and BA2—appeared to alleviate cell membrane stress, with normal erythrocyte morphology and enhanced blood compatibility. The more irregular surface of D caused more hemolysis and platelet aggregation, which was confirmed by hemolysis index and SEM observation. 400 μm blood smears in 10 fields under observation also supported the results.

Overall, hemocompatibility was strongly influenced by surface characteristics, with smoother surfaces (A, B, AA1, BA2) demonstrating superior blood compatibility. These findings highlight the critical role of surface smoothness in optimizing hemocompatibility for blood-contact applications, reinforcing the need to meet ISO 10993-4 standards for safe clinical use.

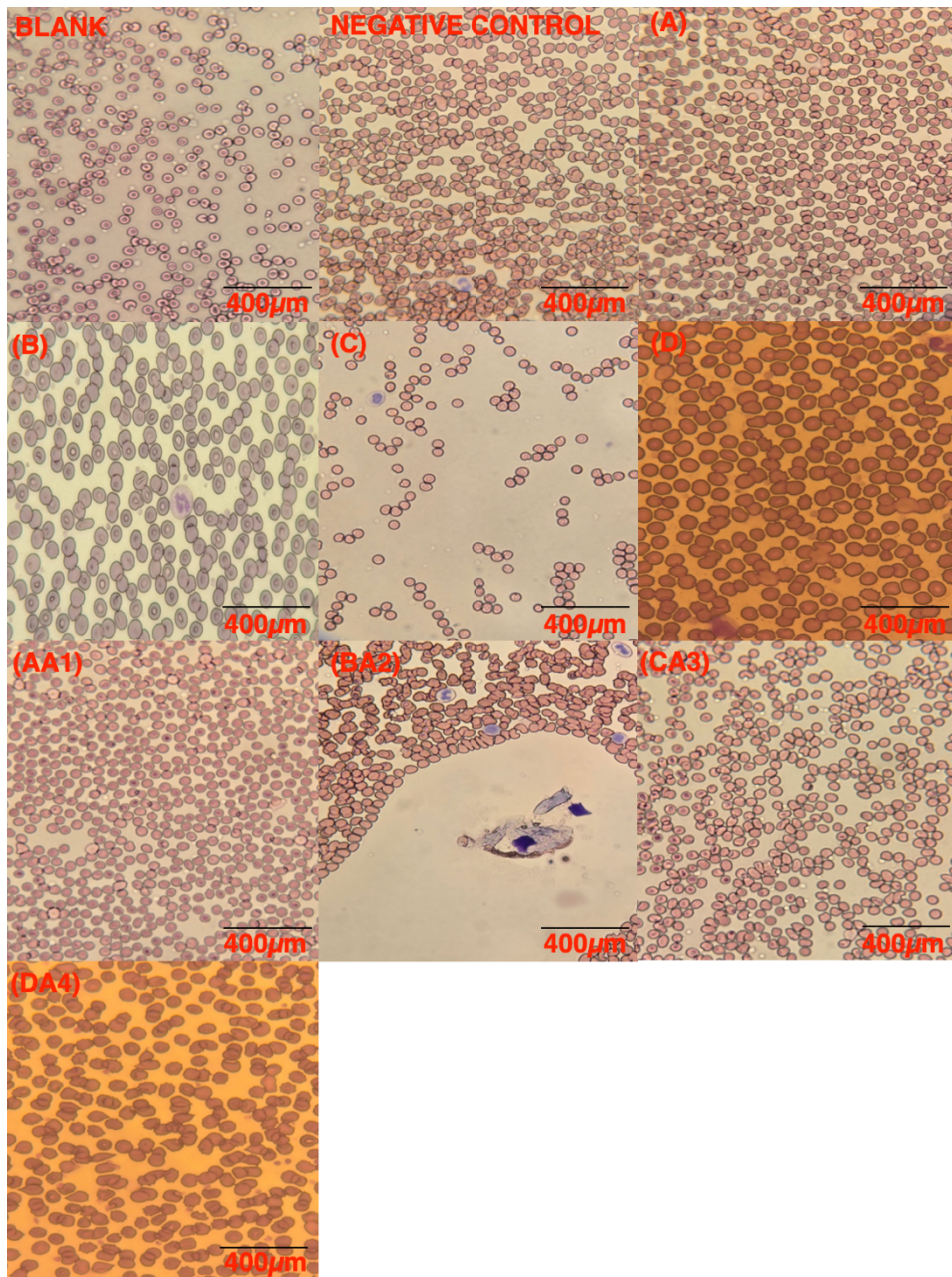


Figure 13

Peripheral blood smears

Figure 13 illustrates the analysis of peripheral blood smears for erythrocyte morphology and platelet adhesion, conducted on blank samples, negative controls, and hydrogel-treated blood samples, all observed at a magnification of 400 µm.

5. CHAPTER V

Discussion

In this present research work, different concentrations of gellan gum (0.3%, 0.5%, 0.75%, and 1%) were mixed with silk fibroin (3%) and separately with sodium alginate (4.2%). This choice was significant as it allowed us to investigate the mechanical and biological characteristics of such blends, which have not been extensively investigated so far. Interestingly, no direct comparisons are found in the literature for gellan gum-silk fibroin and gellan gum-alginate blends at these particular concentrations. Furthermore, to our knowledge, neither of these types of blends has ever been thoroughly evaluated for their impact on mESC or their hemocompatibility. Through exploration of these aspects, we hope to offer new insight into biomaterial science and, at best, discover new applications or upgrades on existing biomaterial formulations. Comparison to existing work helps to characterize our research's unique focus on these specific blend compositions and biological testing, thereby adding to the field's understanding of their potential biomedical applications.

In contrast to earlier studies that focused on single-component biomaterials or different blend ratios, our research extends this foundation by systematically examining the effect of gellan gum at different concentrations (0.3%, 0.5%, 0.75%, and 1%) in combination with silk fibroin and separately with alginate. This approach is derived from the work of S. Lee et al., (2021) by comparing the exact compositions of blends directly, which were not extensively researched previously. Furthermore, though S. Lee et al., (2021) researched similar biomaterials, they never examined the mESC-specific uses or comprehensive hemocompatibility tests, which are subjects explored within this work to further explain and potential uses for these blends of biomaterials.

The importance of testing biomaterials at various pH levels in an effort to study their stability and functionality in diverse biological environments was highlighted by Silva-Correia et al., (2011) This principle has since been further applied in our current research, where swelling kinetics of our gellan gum-based materials at pH 7.4 and pH 1.2 is specifically studied. This comparative approach not only helps to place in relief the ultimate significance of wide pH characterization but also operates to emphasize our dedication to biomaterial design

innovation for applications demanding toughness in a diverse set of physiological environments. Extending Silva-Correia et al., (2011) preliminary work, our study contributes to the literature on biomaterial behavior in different pH conditions, providing essential information to enable the creation of more durable and cross-functional medical materials.

Our sample testing in both pH 1.2 and pH 7.4 contributes to traditional biomaterial research testing only at physiologic pH 7.4 in an attempt to deliver cell culture and blood compatibility. While pH 7.4 is a norm for biologic application, our inclusion of pH 1.2 is an extension to stress the material to function in more extreme acidic conditions. This comparative study allows us to examine the material's response to pH excursions mimicking hostile physiological milieus, e.g., acidic gastric fluid or local inflammatory tissues. Such findings are very important in the design of biomaterials that can be used efficiently for a broad range of clinical applications, e.g., tissue engineering scaffolds and drug delivery systems for site targeting.

Through the observation of the interaction between pH media and biomaterials, we further understand its biocompatibility. We are dedicated to the scientific validity of our findings, placing them at the cutting edge of biomaterial science, with reflective data useful in the optimization of design and biomedical science research innovation. Hydrogels were, in this work, verified to be swellable in PBS more than ABS. Hydrogels in this study were more swellable in PBS compared to ABS because of the high pH nature of PBS which favors ionization and electrostatic repulsion of the hydrogel. This is in line with Mouser et al., (2016), which also found more swelling in basic to neutral pH conditions compared to acidic conditions.

The results revealed that silk fibroin hydrogels were less swollen and more stable than sodium alginate hydrogels. This was because the silk fibroin was more crosslinked, thus being stronger and more resistant to swelling. This is in agreement with Kim et al., (2004), where hydrogels formed from silk fibroin were found to be mechanically stronger and swelling was repressed due to stable β -sheet structures.

Higher gellan gum concentration lowered swelling capacity as a result of denser crosslinking and smaller pore size. This is also reported by Mouser et al., (2016) who reported the same with higher polymer concentration leading to denser networks that limit water imbibition.

These facts, as usual for other experiments, demonstrate that buffer composition, form of the biomaterial, and polymer concentration influence hydrogel swelling, required for the optimization of hydrogel design in biomedical applications.

This study comprehensively assessed hydrogel performance in cell culture experiments with STO cells and mESCs. Oliveira et al. (2010) analyzed cell morphology and other cellular behaviors, viability dynamics, and cytotoxicity by LDH assays and concluded that it gave valuable information regarding their suitability for biomedical applications.

G. H. Kim et al., (2012) examined the fibroblastic morphology of mESCs and the mESCs' colony formation specifically in all hydrogel samples. These materials were observed to maintain cellular morphology even after mitomycin C treatment, indicating their capacity to maintain cellular integrity during experimental durations.

Variations in cell viability for the hydrogel samples were noted during the experimental time. BA2 and CA3 were initially the same on day 1, and they exhibited superior cell viability on days 4 and 7 compared to AA1, B, C, and D. The results support that BA2 and CA3 are an environment that is favorable to sustaining and enhancing cellular activity with time. G. H. Kim et al., (2012) results highlight the significance of selecting the most appropriate material in order to achieve the best of experimental outcomes.

Oliveira et al., (2010) have also conducted LDH cytotoxicity assays to identify BA2 and C materials with reduced cytotoxicity rates than others. This indicates reduced disruption to cell membrane integrity and cell health in general, further indicating BA2 and C as high biocompatibility materials for cell culture use.

BA2, AA1, and C material compositions were examined as to how it affects the later performance in cell culture.

BA2 with 4.2% sodium alginate and 0.5% gellan gum, AA1 with equal quantity but in reduced ratio of gellan gum, and C with the incorporation of 0.5% gellan gum and 3% silk fibroin, as far as biocompatibility and cellular activity are concerned, blends differ on their merits. These findings show that gellan gum, sodium alginate, and silk fibroin have a synergistic effect of cell morphology and viability maintenance excellent during extended periods of culturing. Enhanced cell culture performance of BA2, AA1, and C biomaterials will bring striking effects to further biomedical science and applications. The research confirms the effectiveness of the materials against the reduction of cell viability and cytotoxicity with humongous potential for them to be applied in their eventual use in regenerative medicine and tissue bioengineering research studies. BA2, AA1, and C materials exhibit effective characteristics of maintenance of cell viability, morphological integrity, and the reduction of the cytotoxic effect.

DSC analysis is one of the most significant analysis methods for assessing thermal properties of hydrogels, particularly those made from gellan gum. DSC analysis provides valuable information on thermal transitions such as peak temperatures with direct relevance to the stability, integrity, and potential application of hydrogels in biomedicine. These thermal properties are relevant to the prediction of hydrogel behavior under physiological conditions, i.e., biocompatibility and functionality in cell culture systems.

Two of the gellan gum hydrogels, Sample C and Sample BA2, were chosen from our study because they showed high performance when used in cell culture. Alternatively, two of the hydrogels with undesirable swelling kinetics, i.e., Sample D and Sample DA4, were chosen for comparative purposes.

Gellan gum is generally well recognized to be thermomutability and solid gel-forming character that impacts maximum temperatures tolerated by hydrogels (Vieira et al., 2021). Use of gellan gum will rather enhance general heat resistance of a matrix in a hydrogel producing greater peak temperatures.

Silk fibroin addition also lowers the peak temperature compared to the pure gellan gum systems. Silk fibroin is incorporated into the hydrogel matrix, showing flexibility and

biocompatibility to enhance cell adhesion and growth (Dong et al., 2015). Sample C, for example, contained a lower peak temperature of 58.41°C, an indicator of increased incorporation and homogeneity and appropriateness for use in cell cultures.

Concurrently, the sodium alginate addition would also rise peak temperature as seen from Sample BA2 (76.54°C) and Sample DA4 (79.30°C). Sodium alginate will generate heat-resistant firmer network within gellan gum matrix that will reduce porosity and flexibility and impair cell culture performance.

Generally, gellan gum will exhibit heat transitions between 80°C and 120°C depending upon concentration and additive dependence. Alginate hydrogels will generally exhibit maxima between 70°C and 90°C, and silk fibroin hydrogels will generally exhibit transitions between 50°C and 80°C depending upon their relative biocompatibility and flexibility.

Our DSC studies of hydrogels of gellan gum show that thermal properties of hydrogels are regulated by which additive is used (alginate or silk fibroin).

Lower peak temperature values of hydrogels, indicating higher integration and homogeneity within the matrix, are shown to exhibit better performance under cell culture with focus on higher biocompatibility and biomedical application (Kumar et al., 2016). Gellan gum also has an appropriate thermal backbone but certain additives such as silk fibroin and sodium alginate can influence the top temperatures and therefore hydrogel performance during cell culture (Morris et al., 2012). As opposed to in our work in accordance with Lee et al.'s (2021) study comparing gellan gum-based hydrogels which differ based on additives.

Lee et al., (2021) also observed that silk fibroin-loaded hydrogels have lower peak temperatures, a reflection of higher matrix incorporation and homogeneity similar to our finding in Sample C. The two other studies confirmed that the sodium alginate-loaded hydrogels tend to have higher peak temperatures as a result of stiffer network formed in the gellan gum matrix similar to our finding in Sample BA2 and DA4. Lee et al., (2021) study on the different concentrations of gellan gum, sodium alginate and silk fibroin also confirms our understanding on how these preparations affect thermal stability and swelling behavior necessary for effective hydrogel design in biomedical applications.

Thermal characterization of certain hydrogel samples reveals the significant role played by silk fibroin and sodium alginate additives in altering the thermal characteristics and nature of gellan gum-based hydrogels. The comparative method serves to establish the hydrogel's behavior, which ends up in the synthesis of biomaterials that are well engineered for biomedical applications.

The SEM micrographs exhibit typical surface morphologies of the six hydrogel scaffolds and the main contribution of variance is due to gellan gum, sodium alginate and silk fibroin concentration. Every hydrogel has different topographical features, which are accounted by ratios of three component mixing.

Hydrogel DA4 possesses the most complicated surface with a strongly porous structure that contains major roughness. The above conclusion agrees with the Akkineni et al. (2016) study, where greater amounts of gellan gum and sodium alginate concentration have been shown to form hydrogels with an interconnected network, dense and more solid structure. Such a structure is useful when used, e.g., in drug delivery or tissue scaffolding, since in such cases porosity as well as strength are major criteria.

Further research could include the mechanical and biological properties of these hydrogels with a more detailed research into their applications in the field of regenerative medicine in the future.

For our hemocompatibility experiment, Samples BA2, AA1, and C were investigated to study their interaction with blood constituents in terms of coagulation parameters, CBC, hemolysis, erythrocyte morphology, and platelet adhesion.

In vitro, coagulation tests also showed that the samples BA2, AA1, and C did not have any effect on major coagulation parameters, such as PT, aPTT, and fibrinogen level.

The finding is consistent with that of Gaharwar et al. (2014), where they showed that hydrogel materials are able to preserve hemostatic integrity without interfering with key clotting factors in blood coagulation. Additionally, Gaharwar et al., (2014) demonstrated that

these materials significantly reduced *in vitro* blood clotting times were reduced by 77%, and also increased stable clot formation. The study by Rastogi & Kandasubramanian, (2019) investigated the fibroblastic morphology of STO cells and the evident colony formation of mESCs on all the hydrogel samples. Studies demonstrated that the materials sustained cellular morphology even upon treatment with mitomycin C, which proved their capacity to uphold cellular integrity during experimental conditions.

Hemocompatibility of gellan gum hydrogels is closely linked to their surface characteristics, which are critical for blood interaction and overall compatibility, which determine blood component interactions. Hydrogels with smoother surfaces exhibited reduced platelet adhesion and reduced coagulation and hemolysis risks, while rough surfaces correlated with increased platelet aggregation and thrombotic response. Optimizing the surface is emphasized, particularly in the potential application for vascular grafts and other biomedical implants.

CBC determination (Table 3) confirmed that hydrogel-treated blood samples remained to possess major parameters in medically acceptable ranges.

Hemoglobin concentration and cell indices, MCH and MCV, remained unchanged with no adverse influence on blood cell structure or function. Erythrocyte morphology tests again confirmed these observations, with hydrogels preserving cell structure without deformation or lysis. Peripheral blood smear analysis (Figure 13) revealed that smoother hydrogel surfaces, e.g., in 0.3%–0.5% gellan gum formulations, minimized membrane stress and maintained normal erythrocyte morphology. Coagulation testing (Table 4) revealed that all hydrogel specimens maintained PT, aPTT, and fibrinogen at normal levels, maintaining hemostatic homeostasis. Material composition-dependent distinctions were silk fibroin-derived hydrogels with increased clotting times, this suggests potential activation of the extrinsic coagulation pathway, and sodium alginate-derived hydrogels with slowed clotting and lower fibrinogen, suggesting slowed intrinsic pathway activation. These differences indicate the value of material composition in regulating coagulation response for specific clinical application.

The hemolysis index (Table 5) was within limits for all of the formulations, confirming their blood compatibility.

Smaller gellan gum levels (0.3%–0.5%) exhibited minimal hemolysis, whereas the upper levels (0.75%–1%) exhibited relatively high indices, which are likely attributable to increased surface roughness. Although the hemolysis varied with increased amounts of gellan gum, overall values were mild and suggested these hydrogels remain deserving of blood-contact application. The results underscore the need for accurate polymer concentration adjustment for maximum compatibility. Platelet adhesion study also established the function of surface properties.

Hydrogels with smoother surfaces such as 0.3% and 0.5% gellan gum showed minimal platelet aggregation, exhibiting better blood compatibility. Formulations with 0.75% and 1% gellan gum, however, showed localized platelet aggregation, which was caused by higher surface roughness. SEM imaging confirmed these findings, highlighting the role of smoother surfaces in reducing platelet interaction and enhancing hemocompatibility. BA2, AA1, and C samples had good hemocompatibility profiles in this research, as they did in previous work demonstrating them to be suitable for biomedical applications involving blood contact.

6. CHAPTER VI

Conclusion and recommendations

In the current thesis, we have extensively examined gellan gum-based biomaterials, blended with silk fibroin and alginate at various concentrations, to enhance their properties, biological interactions, and suitability in biomedical applications. Our study fills some significant voids in available information on such biomaterial blends in terms of how they function under different physiological conditions and how they interact with biological systems.

The study began with an evaluation of some physio-chemical characteristics of gellan gum hydrogels. By mixing sodium alginate and silk fibroin at 0.3% to 1% concentrations, we systematically explored the influence of these additives on the stiffness, swelling behavior, and thermal stability of the hydrogels. DSC analysis revealed distinct thermal transitions based on the nature and concentration of additives, which suggested the structural integrity and possible biomedical applications of the hydrogels.

At the center of our studies was the investigation of such biomaterial blends in biological environments. We conducted comprehensive cell culture experiments using mESCs and STO cells to examine biocompatibility, cytotoxicity, and the capability of sustaining cellular proliferation and morphology over long time frames. BA2, AA1, and C samples were particularly interesting ones with much higher cell viability and morphology compared to other samples. These results underscore the significant potential of these blends in driving tissue engineering and regenerative medicine applications, where it is critically important to maintain cellular integrity and function.

Appreciating the role of the environment in biomaterial performance, we broadened conventional pH characterization to encompass measurements at pH 7.4 and pH 1.2. This led us to understand how the changes in pH influence hydrogel swelling kinetics, giving valuable insights into their stability in physiological and acidic environments. Such thorough pH characterization is absolutely necessary for the development of biomaterials that are

resistant to dynamic biological environments, thus making them practically useful in various clinical applications.

In addition, our research explored the hemocompatibility of these biomaterial blends by evaluating their interaction with blood constituents using coagulation tests, hemolysis experiments, and erythrocyte morphology analysis. BA2, AA1, and C samples had little effect on blood clotting factors and erythrocyte viability, implicating their suitability for use in direct blood contact applications, for example, implantable devices and wound dressings.

In conclusion, this thesis has a major contribution to biomaterial science by advancing the understanding of gellan gum-based blends with silk fibroin and alginate. From comprehensive mechanical, biological, thermal, and hemocompatibility tests, we have established the significant features that influence their performance and applicability in biomedical purposes. Our findings highlight the importance of tailor-made biomaterials that can support cellular activity, adapt to physiological conditions, and circumvent futile biological interactions. Future research may include other additives, optimize blend compositions, and utilize these findings for successful biomedical breakthroughs to benefit patient care and outcome.

By answering these research objectives, this thesis not just contributes to the fundamental knowledge of biomaterials but also gives the foundation for future development in biomaterial design, laying down the groundwork for more efficient therapeutic interventions and innovation in biomedical technology.

REFERENCES

- Aamodt, J. M., & Grainger, D. W. (2016). Extracellular matrix-based biomaterial scaffolds and the host response. *Biomaterials*, *86*, 68–82.
<https://doi.org/https://doi.org/10.1016/j.biomaterials.2016.02.003>
- Adalı, T., & Uncu, M. (2016). Silk fibroin as a non-thrombogenic biomaterial. *International Journal of Biological Macromolecules*, *90*, 11–19.
<https://doi.org/10.1016/j.ijbiomac.2016.01.088>
- Akkineni, A. R., Ahlfeld, T., Funk, A., Waske, A., Lode, A., & Gelinsky, M. (2016). Highly concentrated alginate-gellan gum composites for 3D plotting of complex tissue engineering scaffolds. *Polymers*, *8*(5), 170.
- Andersen, T., Auk-Emblem, P., & Dornish, M. (2015). 3D Cell Culture in Alginate Hydrogels. *Microarrays*, *4*(2), 133–161. <https://doi.org/10.3390/microarrays4020133>
- Bhatia, S., & Bhatia, S. (2016). Natural polymers vs synthetic polymer. *Natural Polymer Drug Delivery Systems: Nanoparticles, Plants, and Algae*, 95–118.
- Braune, S., Grunze, M., Straub, A., & Jung, F. (2013). *Are there sufficient standards for the in vitro hemocompatibility testing of biomaterials?*
<http://www.biointerphases.com/content/8/1/33>
- Burdick, J. A., & Prestwich, G. D. (2011). Hyaluronic acid hydrogels for biomedical applications. *Advanced Materials*, *23*(12). <https://doi.org/10.1002/adma.201003963>
- Carrêlo, H., Cidade, M. T., Borges, J. P., & Soares, P. (2023). Gellan gum/alginate microparticles as drug delivery vehicles: DOE production optimization and drug delivery. *Pharmaceuticals*, *16*(7), 1029.
- Ciocchi, M., Cacciotti, I., Seliktar, D., & Melino, S. (2018). Injectable silk fibroin hydrogels functionalized with microspheres as adult stem cells-carrier systems. *International Journal of Biological Macromolecules*, *108*, 960–971.
<https://doi.org/10.1016/j.ijbiomac.2017.11.013>
- da Silva, L. P., Cerqueira, M. T., Sousa, R. A., Reis, R. L., Correlo, V. M., & Marques, A. P. (2014). Engineering cell-adhesive gellan gum spongy-like hydrogels for regenerative medicine purposes. *Acta Biomaterialia*, *10*(11), 4787–4797.
- Dong, Y., Dong, P., Huang, D., Mei, L., Xia, Y., Wang, Z., Pan, X., Li, G., & Wu, C. (2015). Fabrication and characterization of silk fibroin-coated liposomes for ocular drug delivery. *European Journal of Pharmaceutics and Biopharmaceutics*, *91*, 82–90.
- Gaharwar, A. K., Avery, R. K., Assmann, A., Paul, A., McKinley, G. H., Khademhosseini, A., & Olsen, B. D. (2014). Shear-thinning nanocomposite hydrogels for the treatment of hemorrhage. *ACS Nano*, *8*(10), 9833–9842. <https://doi.org/10.1021/nn503719n>
- Gao, W., Wang, H., Liu, Y., Tang, Q., Wu, P., Lin, T., Li, T., & Sun, D. (2022). Sodium alginate-hydrogel coatings on extracorporeal membrane oxygenation for anticoagulation. *Frontiers in Cardiovascular Medicine*, *9*, 966649.
- Gibson, W., & Sanderson, G. R. (1997). Gellan gum. In *Thickening and gelling agents for food* (pp. 119–143). Springer.
- Hang, Y., Ma, X., Liu, C., Li, S., Zhang, S., Feng, R., Shang, Q., Liu, Q., Ding, Z., Zhang, X., Yu, L., Lu, Q., Shao, C., Chen, H., Shi, Y., He, J., & Kaplan, D. L. (2021). Blastocyst-Inspired Hydrogels to Maintain Undifferentiation of Mouse Embryonic Stem Cells. *ACS Nano*, *15*(9), 14162–14173. <https://doi.org/10.1021/acsnano.0c10468>

- Huang, M., & Yang, M. (2010). Swelling and biocompatibility of sodium alginate/poly (γ -glutamic acid) hydrogels. *Polymers for Advanced Technologies*, 21(8), 561–567.
- Ibrahim, H. K., Abdel Malak, N. S., & Abdel Halim, S. A. (2015). Formulation of Convenient, Easily Scalable, and Efficient Granisetron HCl Intranasal Droppable Gels. *Molecular Pharmaceutics*, 12(6), 2019–2025. <https://doi.org/10.1021/mp500825n>
- Jin, Z.-B., Gao, M.-L., Deng, W.-L., Wu, K.-C., Sugita, S., Mandai, M., & Takahashi, M. (2019). Stemming retinal regeneration with pluripotent stem cells. *Progress in Retinal and Eye Research*, 69, 38–56.
- Kannan, R., Wei, G., & Ma, P. X. (2022). Synthetic polymeric biomaterials for tissue engineering. In *Tissue Engineering Using Ceramics and Polymers* (pp. 41–74). Elsevier.
- Kim, G. H., Lee, G. R., Choi, H. I., Park, N. H., Chung, H. T., & Han, I. S. (2012). Overexpression of bone morphogenetic protein 4 in STO fibroblast feeder cells represses the proliferation of mouse embryonic stem cells *in vitro*. *Experimental and Molecular Medicine*, 44(7), 457–463. <https://doi.org/10.3858/emm.2012.44.7.052>
- Kim, U.-J., Park, J., Li, C., Jin, H.-J., Valluzzi, R., & Kaplan, D. L. (2004). Structure and Properties of Silk Hydrogels. *Biomacromolecules*, 5(3), 786–792. <https://doi.org/10.1021/bm0345460>
- Kumar, A., Nune, K. C., Murr, L. E., & Misra, R. D. K. (2016). Biocompatibility and mechanical behaviour of three-dimensional scaffolds for biomedical devices: process–structure–property paradigm. *International Materials Reviews*, 61(1), 20–45.
- Lalebeigi, F., Alimohamadi, A., Afarin, S., Aliabadi, H. A. M., Mahdavi, M., Farahbakhshpour, F., Hashemiaval, N., Khandani, K. K., Eivazzadeh-Keihan, R., & Maleki, A. (2024). Recent advances on biomedical applications of gellan gum: A review. In *Carbohydrate Polymers* (Vol. 334). Elsevier Ltd. <https://doi.org/10.1016/j.carbpol.2024.122008>
- Lee, S., Choi, J., Youn, J., Lee, Y., Kim, W., Choe, S., Song, J., Reis, R. L., & Khang, G. (2021a). Development and evaluation of gellan gum/silk fibroin/chondroitin sulfate ternary injectable hydrogel for cartilage tissue engineering. *Biomolecules*, 11(8), 1184.
- Lee, S., Choi, J., Youn, J., Lee, Y., Kim, W., Choe, S., Song, J., Reis, R. L., & Khang, G. (2021b). Development and evaluation of gellan gum/silk fibroin/chondroitin sulfate ternary injectable hydrogel for cartilage tissue engineering. *Biomolecules*, 11(8). <https://doi.org/10.3390/biom11081184>
- Morris, E. R., Nishinari, K., & Rinaudo, M. (2012). Gelation of gellan—a review. *Food Hydrocolloids*, 28(2), 373–411.
- Mouser, V. H. M., Melchels, F. P. W., Visser, J., Dhert, W. J. A., Gawlitta, D., & Malda, J. (2016). Yield stress determines bioprintability of hydrogels based on gelatin-methacryloyl and gellan gum for cartilage bioprinting. *Biofabrication*, 8(3), 035003.
- Moyo, M. T. G., & Adali, T. (2024). Gellan gum as a promising transplantation carrier for differentiated progenitor cells in ophthalmic therapies. *Journal of Bioactive and Compatible Polymers*, 0(0), 08839115241278739. <https://doi.org/10.1177/08839115241278739>
- Moyo, M. T. G., Adali, T., & Edebal, O. H. (2024). ISO 10993-4 Compliant Hemocompatibility Evaluation of Gellan Gum Hybrid Hydrogels for Biomedical Applications. *Gels*, 10(12), 824.
- Moyo, M. T. G., Adali, T., & Tulay, P. (2024). Exploring gellan gum-based hydrogels for regenerating human embryonic stem cells in age-related macular degeneration therapy: A literature review. *Regenerative Therapy*, 26, 235–250.

- Moyo, M. T. G., Adali, T., Edebal, O. H., Bayir, E., & Şendemir, A. (2023). HEMOCOMPATIBILITY STUDIES OF LAYER-BY-LAYER POLYELECTROLYTE COMPLEXES FOR BIO-BASED POLYMERS. *Materials and Technology*, 57(5), 525–536.
- Na, K. S., Fernandes-Cunha, G. M., Varela, I. B., Lee, H. J., Seo, Y. A., & Myung, D. (2021). Effect of mesenchymal stromal cells encapsulated within polyethylene glycol-collagen hydrogels formed in situ on alkali-burned corneas in an ex vivo organ culture model. *Cytotherapy*, 23(6), 500–509. <https://doi.org/10.1016/j.jcyt.2021.02.001>
- Oliveira, J. T., Gardel, L. S., Rada, T., Martins, L., Gomes, M. E., & Reis, R. L. (2010). Injectable gellan gum hydrogels with autologous cells for the treatment of rabbit articular cartilage defects. *Journal of Orthopaedic Research*, 28(9), 1193–1199. <https://doi.org/10.1002/jor.21114>
- Osmałek, T., Froelich, A., & Tasarek, S. (2014). Application of gellan gum in pharmacy and medicine. In *International Journal of Pharmaceutics* (Vol. 466, Numbers 1–2, pp. 328–340). Elsevier B.V. <https://doi.org/10.1016/j.ijpharm.2014.03.038>
- Palumbo, F. S., Federico, S., Pitarresi, G., Fiorica, C., & Giammona, G. (2020). Gellan gum-based delivery systems of therapeutic agents and cells. In *Carbohydrate Polymers* (Vol. 229). Elsevier Ltd. <https://doi.org/10.1016/j.carbpol.2019.115430>
- Paulsson, M., Hägerström, H., & Edsman, K. (1999). Rheological studies of the gelation of deacetylated gellan gum (Gelrite®) in physiological conditions. *European Journal of Pharmaceutical Sciences*, 9(1), 99–105.
- Payne, C., Dolan, E. B., O’Sullivan, J., Cryan, S. A., & Kelly, H. M. (2017). A methylcellulose and collagen based temperature responsive hydrogel promotes encapsulated stem cell viability and proliferation *in vitro*. *Drug Delivery and Translational Research*, 7(1), 132–146. <https://doi.org/10.1007/s13346-016-0347-2>
- Raghavendra, G. M., Varaprasad, K., & Jayaramudu, T. (2015). Biomaterials: design, development and biomedical applications. In *Nanotechnology applications for tissue engineering* (pp. 21–44). Elsevier.
- Rastogi, P., & Kandasubramanian, B. (2019). Review of alginate-based hydrogel bioprinting for application in tissue engineering. *Biofabrication*, 11(4), 42001. <https://doi.org/10.1088/1758-5090/ab331e>
- Rim, M. A., Choi, J. H., Park, A., Youn, J., Lee, S., Kim, N. E., Song, J. E., & Khang, G. (2020). Characterization of gelatin/gellan gum/glycol chitosan ternary hydrogel for retinal pigment epithelial tissue reconstruction materials. *ACS Applied Bio Materials*, 3(9), 6079–6087.
- Seo, J. S., Tumursukh, N.-E., Choi, J. H., Song, Y., Jeon, G., Kim, N. E., Kim, S. J., Kim, N., Song, J. E., & Khang, G. (2023). Modified gellan gum-based hydrogel with enhanced mechanical properties for application as a cell carrier for cornea endothelial cells. *International Journal of Biological Macromolecules*, 236, 123878.
- Seyfert, U. T., Biehl, V., & Schenk, J. (2002). *In vitro* hemocompatibility testing of biomaterials according to the ISO 10993-4. *Biomolecular Engineering*, 19(2–6), 91–96.
- Silva-Correia, J., Oliveira, J. M., Caridade, S. G., Oliveira, J. T., Sousa, R. A., Mano, J. F., & Reis, R. L. (2011). Gellan gum-based hydrogels for intervertebral disc tissue-engineering applications. *Journal of Tissue Engineering and Regenerative Medicine*, 5(6). <https://doi.org/10.1002/term.363>

- Sodunke, T. R., Turner, K. K., Caldwell, S. A., McBride, K. W., & Reginato, M. J. (2007). Micropatterns of Matrigel for three-dimensional epithelial cultures. *Biomaterials*, *28*(27), 4006–4016.
- Sperling, C., Schweiss, R. B., Steller, U., & Werner, C. (2005). *In vitro* hemocompatibility of self-assembled monolayers displaying various functional groups. *Biomaterials*, *26*(33), 6547–6557.
- Stachowiak, N., Kowalonek, J., Kozłowska, J., & Burkowska-But, A. (2023). Stability Studies, Biodegradation Tests, and Mechanical Properties of Sodium Alginate and Gellan Gum Beads Containing Surfactant. *Polymers*, *15*(11), 2568.
- Tardy, B. L., Mattos, B. D., Otoni, C. G., Beaumont, M., Majoinen, J., Kämäräinen, T., & Rojas, O. J. (2021). Deconstruction and reassembly of renewable polymers and biocolloids into next generation structured materials. *Chemical Reviews*, *121*(22), 14088–14188.
- Tsaryk, R., Silva-Correia, J., Oliveira, J. M., Unger, R. E., Landes, C., Brochhausen, C., Ghanaati, S., Reis, R. L., & Kirkpatrick, C. J. (2017). Biological performance of cell-encapsulated methacrylated gellan gum-based hydrogels for nucleus pulposus regeneration. *Journal of Tissue Engineering and Regenerative Medicine*, *11*(3), 637–648. <https://doi.org/10.1002/term.1959>
- Vieira, S., da Silva Morais, A., Garet, E., Silva-Correia, J., Reis, R. L., Gonzalez-Fernandez, A., & Oliveira, J. M. (2021). Methacrylated gellan gum/poly-l-lysine polyelectrolyte complex beads for cell-based therapies. *ACS Biomaterials Science & Engineering*, *7*(10), 4898–4913.
- Vuorenää, H., Valtonen, J., Penttinen, K., Koskimäki, S., Hovinen, E., Ahola, A., Gering, C., Parraga, J., Kelloniemi, M., & Hyttinen, J. (2024). Gellan gum-gelatin based cardiac models support formation of cellular networks and functional cardiomyocytes. *Cytotechnology*, 1–20.
- Wang, T., Yi, W., Zhang, Y., Wu, H., Fan, H., Zhao, J., & Wang, S. (2023). Sodium alginate hydrogel containing platelet-rich plasma for wound healing. *Colloids and Surfaces B: Biointerfaces*, *222*, 113096.
- Weber, M., Steinle, H., Golombek, S., Hann, L., Schlensak, C., Wendel, H. P., & Avcı-Adalı, M. (2018). Blood-Contacting Biomaterials: *In Vitro* Evaluation of the Hemocompatibility. In *Frontiers in Bioengineering and Biotechnology* (Vol. 6). Frontiers Media S.A. <https://doi.org/10.3389/fbioe.2018.00099>
- Wong, F. S. Y., Tsang, K. K., Chu, A. M. W., Chan, B. P., Yao, K. M., & Lo, A. C. Y. (2019). Injectable cell-encapsulating composite alginate-collagen platform with inducible termination switch for safer ocular drug delivery. *Biomaterials*, *201*, 53–67. <https://doi.org/https://doi.org/10.1016/j.biomaterials.2019.01.032>
- Wu, S., Xiao, R., Wu, Y., & Xu, L. (2024). Advances in tissue engineering of gellan gum-based hydrogels. In *Carbohydrate Polymers* (Vol. 324). Elsevier Ltd. <https://doi.org/10.1016/j.carbpol.2023.121484>

APPENDIX A Similarity report

M Moyo Thesis

ORJİNALLIK RAPORU

% 10	% 8	% 6	%
BENZERLİK ENDEKSİ	İNTERNET KAYNAKLARI	YAYINLAR	ÖĞRENCİ ÖDEVLERİ

BİRİNCİL KAYNAKLAR

1	www.mdpi.com İnternet Kaynağı	% 6
2	Mthabisi Talent George Moyo, Terin Adali, Oğuz Han Edebal. "ISO 10993-4 Compliant Hemocompatibility Evaluation of Gellan Gum Hybrid Hydrogels for Biomedical Applications", Gels, 2024 Yayın	% 1
3	Khawaja Husnain Haider. "Handbook of Regenerative Medicine - Cell-Free Therapy Approach", CRC Press, 2025 Yayın	<% 1
4	www.frontiersin.org İnternet Kaynağı	<% 1
5	scholarworks.iupui.edu İnternet Kaynağı	<% 1
6	Ying Wei, Uwimana Alexandre, Xiang Ma. "Hydrogels to Support Transplantation of Human Embryonic Stem Cell-Derived Retinal Pigment Epithelial Cells", Brain Sciences, 2022 Yayın	<% 1
7	Queeny Dasgupta, Kaushik Chatterjee, Giridhar Madras. "Combinatorial Approach to Develop Tailored Biodegradable Poly(xylitol dicarboxylate) Polyesters", Biomacromolecules, 2014 Yayın	<% 1
8	Costache, M.C., A.D. Vaughan, H. Qu, P. Ducheyne, and D.I. Devore. "Tyrosine-derived polycarbonate-silica xerogel nanocomposites for controlled drug delivery", Acta Biomaterialia, 2013. Yayın	<% 1

9	Surette, M.E.. "Inhibition of leukotriene synthesis, pharmacokinetics, and tolerability of a novel dietary fatty acid formulation in healthy adult subjects", <i>Clinical Therapeutics</i> , 200303 Yayın	<% 1
10	www.spandidos-publications.com İnternet Kaynağı	<% 1
11	bdpsjournal.org İnternet Kaynağı	<% 1
12	epdf.pub İnternet Kaynağı	<% 1
13	ocw.mit.edu İnternet Kaynağı	<% 1
14	shura.shu.ac.uk İnternet Kaynağı	<% 1
15	worldwidescience.org İnternet Kaynağı	<% 1
16	www.ncbi.nlm.nih.gov İnternet Kaynağı	<% 1
17	eprints.gla.ac.uk İnternet Kaynağı	<% 1
18	Yibo Xu, Chuanxin Chen, Peter B. Hellwarth, Xiaoping Bao. "Biomaterials for stem cell engineering and biomanufacturing", <i>Bioactive Materials</i> , 2019 Yayın	<% 1
19	hi.tamu.edu İnternet Kaynağı	<% 1
20	ijpsr.com İnternet Kaynağı	<% 1
21	mdpi-res.com İnternet Kaynağı	<% 1
22	repositorium.sdum.uminho.pt İnternet Kaynağı	<% 1
23	Helge Gehrke, Joanna Pelka, Christian G. Hartinger, Holger Blank et al. "Platinum	<% 1

nanoparticles and their cellular uptake and DNA platination at non-cytotoxic concentrations", Archives of Toxicology, 2011
Yayın

24	cancer-nano.biomedcentral.com İnternet Kaynağı	<% 1
25	dokumen.pub İnternet Kaynağı	<% 1
26	"Laboratory Hematology Practice", Wiley, 2012 Yayın	<% 1
27	baadalsg.inflibnet.ac.in İnternet Kaynağı	<% 1
28	dr.ntu.edu.sg İnternet Kaynağı	<% 1
29	www.coursehero.com İnternet Kaynağı	<% 1
30	www.researchgate.net İnternet Kaynağı	<% 1
31	Haiyun Zhou, Jia Wei, Ziheng Wang, Lin Bai, Qianyu Wang, Yumei Wei, Xiaoxia Hu, Xiaojing Tian, Fumei Zhang. "Anti-osteoporosis properties and regulatory impact on gut microbiota of Yak bone meal in Ovariectomized osteoporotic mice", Food Bioscience, 2025 Yayın	<% 1
32	Jan O. Nehlin. "Strategies for future histocompatible stem cell therapy", Biogerontology, 02/15/2009 Yayın	<% 1
33	John Haycock, Arti Ahluwalia, J. Malcolm Wilkinson. "Cellular In Vitro Testing - Methods and Protocols", Pan Stanford, 2019 Yayın	<% 1
34	Mthabisi Talent George Moyo, Terin Adali, Pinar Tulay. "Exploring gellan gum-based hydrogels for regenerating human embryonic stem cells in age-related macular	<% 1

degeneration therapy: A literature review",
Regenerative Therapy, 2024

Yayın

35 Tate, Courtney Marie. "Structure-function analysis of CXXC finger protein 1", Proquest, 20111108 <% 1
Yayın

36 link.springer.com <% 1
İnternet Kaynağı

37 ojrd.biomedcentral.com <% 1
İnternet Kaynağı

38 phcogj.com <% 1
İnternet Kaynağı

39 www.in.gov <% 1
İnternet Kaynağı

40 Çevik, Merve. "Development of a Natural Tubular Scaffold From Decellularized Parsley Stems to be Used in Vascular Tissue Engineering Applications", Izmir Institute of Technology (Turkey) <% 1
Yayın

Alıntılarını çıkart Kapat
Bibliyografyayı Çıkart Kapat

Eşleşmeleri çıkar Kapat

APPENDIX B CV

CV

1. **Name** : Mthabisi Talent George
2. **Surname** : Moyo
3. **Date of Birth.** : 26 February 1996
4. **Title** : Dr
5. **Affiliation** : Girne American University

Degree	Department	University	Year
Bachelor of Science	Bioengineering	Near East University	2017
Master of Science	Biomedical Engineering	Near East University	2020
Doctor of Philosophy	Biomedical Engineering	Near East University	2025

6. Education History & Transcripts:

6.1 Bachelor of Science

Supervisor: Prof. Dr Terin Adalı

Graduation Project Title: Biofiltration of liquids

6.2 Master of Science Thesis

Supervisor: Prof. Dr Terin Adalı

Thesis Title: Biocompatibility Studies of Layer-By-Layer Polyelectrolyte Complexes for Biomedical Applications

CGPA: 3.86/4.00

Transcript:

Biomaterials for medical diagnosis and therapy	AA
Biomedical micro and nanosystems	AA
Nanotechnology in cancer therapy	AA
Computer-aided diagnostics in medical imaging	BB
Advanced Tissue engineering	AA
Scientific research methods and ethics	AA
Advanced Artificial Organs	AA

6.3 Doctor of Philosophy

Supervisor: Prof. Dr Terin Adalı

Thesis Title: Gellan Gum for Stem Cell Culturing

CGPA: 4.00/4.00

Transcript:

Rational Phytotherapy & Clinical Trials	AA
Clinical Toxicology	AA
Clinical Microbiology	AA
Clinical laboratory technique	AA
Advanced biomechanics	AA

Cell culturing techniques	AA
Molecular pathology	AA
Thesis	Satisfactory

7 Scientific Papers (SCIE)

- Kassahun Alula Akulo, Terin Adali, **Mthabisi Talent George Moyo**, Tulin Bodamyali (2022) “**Intravitreal Injectable Hydrogels for Sustained Drug Delivery in Glaucoma Treatment and Therapy**”. *Polymers*, 14 (12) 2359. DOI: 10.3390/polym14122359
- **M.T.G. Moyo**, T. Adali, O.H. Edebal, E. Bayır, A. Şendemir (2023) “**Hemocompatibility Studies of Layer-by-Layer Polyelectrolyte Complexes for Bio-based Polymers.**” *Materials and Technology*, 57(5) 525. DOI: 10.17222/mit.2023.922 and *Technology*, 57(5) 525. DOI: 10.17222/mit.2023.922. 7.1.19
- **M.T.G. Moyo**, T. Adali, Pinar Tulay (2024) “**Exploring gellan gum-based hydrogels for regenerating human embryonic stem cells in age-related macular degeneration therapy: A literature review.**” *Regenerative Therapy* 26 (2024) 235 -250. DOI:10.1016/j.reth.2024.05.018.
- **Moyo MTG**, Adali T. (2024)“**Gellan gum as a promising transplantation carrier for differentiated progenitor cells in ophthalmic therapies**”. *Journal of Bioactive and Compatible Polymers*. (2024);0(0). doi:10.1177/08839115241278739
- **Moyo, M. T. G.**, Adali, T., & Edebal, O. H. (2024). **ISO 10993-4 Compliant Hemocompatibility Evaluation of Gellan Gum Hybrid Hydrogels for Biomedical Applications.** *Gels*, 10(12), 824. <https://doi.org/10.3390/gels10120824>

8 Papers published in SCOPUS.

- **Moyo, Mthabisi Talent George.** "Unveiling the Absence of a Local Medical Device and Biomaterials Manufacturing Industry in Zimbabwe: A Literature Review." *Health Technology Assessment in Action* 7.2 (2023). DOI: 10.18502/htaa.v7i2.13815

9 Papers published in PubMed.

- **George Moyo, Mthabisi Talent**, Fikret Dirilenoğlu, and Yazgı Köy. "Urachal mucinous cystic tumor of low malignant potential: a report of a rare case with literature review." *Surgical and Experimental Pathology* 6.1 (2023): 18.
- Dirilenoğlu, Fikret, **Mthabisi Talent George Moyo**, and Aslı Kahraman. "Primary intra-axial Ewing sarcoma of the central nervous system: report of a rare case with literature review." *Surgical and Experimental Pathology* 6.1 (2023): 12.

10 International Conferences, Congress and Symposium Presentations and publications.

- Akulo K., Fisseha R., Umar A. U., **Moyo M.T. G.**, Adali T., “**Bilayer & TriLayer Alginate and Silk Fibroin Biofilms: Synthesis, Characterization and Platelet Adhesion Studies**”, 2nd International Biomedical Engineering Congress (IBMEC-2018), North Cyprus, P. 153, 2018.
- Terin Adalı, **Mthabisi Talent George Moyo**, “ **Blood Biocompatibility of Silk Fibroin Based Polyelectrolyte Complexes.**” European Biotechnology Congress 2020.
- **Mthabisi Talent George Moyo**, Terin Adali, Oğuzhan Edebal, Aylin Şendemir (2022) **Hemocompatibility studies of Layer – by – Layer Polyelectrolyte Complexes for Biobased**

Polymers. 8th ICNTC (International Conference on New Trends in Chemistry) Conference 16 – 17 May 2022.

11. Administrative Positions:

ADMINISTRATIVE POSITIONS	INSTITUTION	YEARS
Times Higher Education (THE) Impact Methodology Data Management System Coordinator	Girne American University	02.2025 - Present
Coordinator, Phase 1 Medical Students, Faculty of Medicine	Girne American University	08. 2024 - Present
Assistant Phase Coordinator/Academic Advisor, Phase 1 Medical Students, Faculty of Medicine	Girne American University	01. 2024 - 08.2024
Teaching Assistant, Faculty of Medicine	Girne American University	10. 2023- Present
Website coordinator	Girne American University	10. 2023- Present
Research Scholar, Near East University, Faculty of Engineering	Near East University	02. 2018 - Present
Medical Care Assistant ,	Kolan British Hospital	09. 2022 – 09. 2023
Medical Care Assistant ,	Ikinci Bahar Nursing Home	09. 2021 – 09. 2023

12. Courses offered in the past two years:

Academic Year	Period	Course Name	Semester Hours		Number of Students
			Theoretic	Practical	
2024-2025	Committee 1-4	Medical Biochemistry	95	24	79
2023 -2024	Fall	General Chemistry Lab	-	32	60
		-	-	-	-
	Spring	-	-	-	-
		-	-	-	-
			Committee Hours		
			Theoretic	Practical	
2023 - 2024	Committee 1-4	Medical Biochemistry	95	24	96
	Committee 5	Occupational Health & Safety	20	0	54

-Lectures offered to phase 1, phase 2 and phase 3 medical students.

13. Other Courses/ Certifications

- Occupational Health & Safety | University of Cape Town | EdX | 2024
- Principles of Biochemistry | Harvard Online | EdX | 2024
- Hands-On Stem Cell Culture Workshop Embryonic Stem Cell Culture, Passaging & Formation of Embryoid Bodies | DESAM Research Institute | 2023
- EdX verified certificate for Biomaterials and Biofabrication: Design, Engineering and Innovation. | University of Bayreuth | 2022
- EdX verified certificate for Product Design, Prototyping, and Testing | University System of Maryland | 2022
- Coursera verified certificate for Design and Interpretation of Clinical Trials | Johns Hopkins University | 2022
- EdX verified certificate for Product Management Fundamentals | University System of Maryland | 2022
- International English Language Testing System (IELTS) | 2023
- Healthcare Assistant (Advanced Diploma) | Reed | Oct 2022
- Diploma in Caregiving | Alison, CPD Approved / NVQ - Level 2 | Oct 2022
- Diploma in Nursing & Patient care | Alison, CPD Approved / NVQ - Level 2 | Oct 2022
- Health and Social Care | Reed, NVQ Level 5 Diploma | Oct 2022
- Care Giving Skills - Dementia Care | Alison, CPD Approved / NVQ - Level 2 | Oct 2022
- Elderly Care & Care for the Disabled | Alison, CPD Approved / NVQ - Level 2 | Aug 2022
- Care certificate courses (Standard 1 - 15) | Florence Academy, CPD Approved / NVQ - Level 2 | Aug 2022
- Patient Safety & Quality Improvement: Developing a Systems View. | Johns Hopkins University | Coursera | Sep 2022
- Integrative Nursing | University of Minnesota | Coursera Sep 2022

APPENDIX C

Hemocompatibility ethical approval



YAKIN DOĞU ÜNİVERSİTESİ
BİLİMSEL ARAŞTIRMALAR ETİK KURULU

EK: 1037-2020

ARAŞTIRMA PROJESİ DEĞERLENDİRME RAPORU

Toplantı Tarihi : 23.01.2020
Toplantı No : 2020/76
Proje No :955

Yakin Doğu Üniversitesi Mühendislik Fakültesi öğretim üyelerinden Doç. Dr. Terin Adalı'nın sorumlu araştırmacısı olduğu, YDU/2020/76-955 proje numaralı ve "Hidrojel Ve Polielektrolit Yapılarda Kan Uyumluluğu Çalışmaları" başlıklı proje önerisi kurulumuzca değerlendirilmiş olup, etik olarak uygun bulunmuştur.

- | | |
|-------------------------------------|-----------------|
| 1. Prof. Dr. Rıfıfı Onur | (BAŞKAN) |
| 2. Prof. Dr. Nerin Bahşeciler Önder | (ÜYE) KATILMADI |
| 3. Prof. Dr. Tamer Yılmaz | (ÜYE) KATILMADI |
| 4. Prof. Dr. Şahin Saygı | (ÜYE) |
| 5. Prof. Dr. Şanda Çalı | (ÜYE) |
| 6. Prof. Dr. Nedim Çakır | (ÜYE) |
| 7. Prof. Dr. Nurhan Bayraktar | (ÜYE) |
| 8. Doç. Dr. Nilüfer Galip Çelik | (ÜYE) KATILMADI |
| 9. Doç. Dr. Emil Mammadov | (ÜYE) |
| 10. Doç. Dr. Mehtap Tınazlı | (ÜYE) KATILMADI |

APPENDIX D

Figure 1 publishing license



49 Spadina Ave. Suite 200
Toronto ON M5V 2J1 Canada
www.biorender.com

Confirmation of Publication and Licensing Rights - Open Access

February 12th, 2025

Subscription Type: *Student Plan - Academic*
Agreement number: *HP27WK12LH*
Publisher Name: *Near East University*

Figure Title: *Standards and Tests for Biomaterial Assessment*

Citation to Use: *Created in BioRender. Moyo, M. (2025) <https://BioRender.com/s14u510>*

To whom this may concern,

This document ("Confirmation") hereby confirms that Science Suite Inc. dba BioRender ("BioRender") has granted the following BioRender user: Mthabisi Moyo ("User") a BioRender Academic Publication License in accordance with BioRender's [Terms of Service](#) and [Academic License Terms](#) ("License Terms") to permit such User to do the following on the condition that all requirements in this Confirmation are met:

- 1) publish their Completed Graphics created in the BioRender Services containing both User Content and BioRender Content (as both are defined in the License Terms) in publications (journals, textbooks, websites, etc.); and
- 2) sublicense such Completed Graphics under "open access" publication sublicensing models such as CC-BY 4.0 and more restrictive models, so long as the conditions set forth herein are fully met.

Requirements of User:

- 1) All Completed Graphics to be published in any publication (journals, textbooks, websites, etc.) must be accompanied by the following citation either as a caption, footnote or reference for each figure that includes a Completed Graphic:
"Created in BioRender. Moyo, M. (2025) <https://BioRender.com/s14u510>".
- 2) All terms of the License Terms including all Prohibited Uses are fully complied with. E.g. For Academic License Users, no commercial uses (beyond publication in journals, textbooks or websites) are permitted without obtaining or switching to a BioRender Industry Plan.
- 3) A Reader (defined below) may request that the User allow their figure to be a public template for Readers to view, copy, and modify the figure. It is up to the User to determine what level of access to grant.

Open-Access Journal Readers:

Open-Access journal readers ("Reader") who wish to view and/or re-use a particular Completed Graphic in an Open-Access journal subject to CC-BY sublicensing may do so by clicking on the URL link in the applicable citation for the subject Completed Graphic.

The re-use/modification options below are available after the Reader requests the User to adapt their

APPENDIX E

Figure 2 publishing license



49 Spadina Ave. Suite 200
Toronto ON M5V 2J1 Canada
www.biorender.com

Confirmation of Publication and Licensing Rights - Open Access

April 1st, 2025

Subscription Type: Student Plan - Academic
Agreement number: HJ283FPYRL
Publisher Name: Near East University

Figure Title: ISO 10993-4 hemocompatibility assay steps

Citation to Use: Created in BioRender. Moyo, M. (2025) <https://BioRender.com/yn7paix>

To whom this may concern,

This document ("Confirmation") hereby confirms that Science Suite Inc. dba BioRender ("BioRender") has granted the following BioRender user: Mthabisi Moyo ("User") a BioRender Academic Publication License in accordance with BioRender's [Terms of Service](#) and [Academic License Terms](#) ("License Terms") to permit such User to do the following on the condition that all requirements in this Confirmation are met:

- 1) publish their Completed Graphics created in the BioRender Services containing both User Content and BioRender Content (as both are defined in the License Terms) in publications (journals, textbooks, websites, etc.); and
- 2) sublicense such Completed Graphics under "open access" publication sublicensing models such as CC-BY 4.0 and more restrictive models, so long as the conditions set forth herein are fully met.

Requirements of User:

- 1) All Completed Graphics to be published in any publication (journals, textbooks, websites, etc.) must be accompanied by the following citation either as a caption, footnote or reference for each figure that includes a Completed Graphic:
"Created in BioRender. Moyo, M. (2025) <https://BioRender.com/yn7paix>".
- 2) All terms of the License Terms including all Prohibited Uses are fully complied with. E.g. For Academic License Users, no commercial uses (beyond publication in journals, textbooks or websites) are permitted without obtaining or switching to a BioRender Industry Plan.
- 3) A Reader (defined below) may request that the User allow their figure to be a public template for Readers to view, copy, and modify the figure. It is up to the User to determine what level of access to grant.

Open-Access Journal Readers:

Open-Access journal readers ("Reader") who wish to view and/or re-use a particular Completed Graphic in an Open-Access journal subject to CC-BY sublicensing may do so by clicking on the URL link in the applicable citation for the subject Completed Graphic.

The re-use/modification options below are available after the Reader requests the User to adapt their